Essence of Thermal Analysis to Assess Biodiesel Combustion Performance

Vinay Atgur [1], G. Manavendra [2], Nagaraj R. Banapurmath [3,*], Boggarapu Nageswar Rao [1], Ali A. Rajhi [4], T. M. Yunus Khan [4,*], Chandramouli Vadlamudi [5], Sanjay Krishnappa [5], Ashok M. Sajjan [6] and R. Venkatesh [6]

1   Department of Mechanical Engineering, Koneru Lakshmaiah Education Foundation, Vaddeswaram 522302, India
2   Department of Mechanical Engineering, Bapuji Institute of Engineering and Technology (BIET), Davangere 577055, India
3   Department of Mechanical Engineering, K.L.E. Technological University, BVB Campus, Hubballi 580031, India
4   Department of Mechanical Engineering, College of Engineering, King Khalid University, Abha 61421, Saudi Arabia
5   Aerosapien Technologies, Daytona Beach, FL 32114, USA
6   Department of Chemistry, Centre of Excellence in Material Science, K.L.E. Technological University, BVB Campus, Hubballi 580031, India
*   Correspondence: nr_banapurmath@kletech.ac.in (N.R.B.); yunus.tatagar@gmail.com (T.M.Y.K.)

Abstract: The combustion phenomena are always complex in nature due to the involvement of complex series and parallel reactions. There are various methods that are involved in analyzing combustion phenomena. Viscosity is the first and foremost factor that acts as the DNA of fuel. By evaluating the viscosity, it is possible initially to understand the combustion phenomena. Thermophysical and transport properties are helpful during the intensification of the combustion process. Combustion experiments are economically infeasible and time-consuming processes. Combustion simulations demand excellent computational facilities with detailed knowledge of chemical kinetics. So far, the majority of researchers have focused on analyzing coal combustion phenomena, whereas less work has been carried out on liquid fuels, especially biodiesel combustion analysis. Traditional engine testing provides only performance parameters, and it fails to have oversight of the thermodynamic aspects. The application of thermal analysis methods in combustion research is useful in the design, modeling, and operation of the systems. Such investigations are carried out extensively in the combustor, engine, and process industries. The use of differential scanning calorimetry (DSC) and thermogravimetry (TG) to assess the properties of biofuels has been attracting researchers in recent years. The main objective of this paper is to discuss the application of TGA and DSC to analyze heat flow, enthalpy, thermal stability, and combustion indexes. Moreover, this paper reviews some of the other aspects of the kinetics of combustion, transport properties' evaluation, and combustion simulations for biodiesels and their blends. TG curves indicate two phases of decomposition for diesel and three phases for biofuel. The B-20 blend's (20% biodiesel and 80% diesel) performance was found to be similar to that of diesel with the combustion index and intensity of combustion nearly comparable with diesel. It is thermally more stable with a high offset temperature, confirming a longer combustion duration. A case study reported in this work showed diesel and B20 JOME degradation start from 40 °C, whereas jatropha oil methyl ester (JOME) degradation starts from 140 °C. JOME presents more decomposition steps with high decomposition temperatures, indicative of more stable compound formation due to the oxidation process. The peak temperature of combustion for diesel, JOME, and B20 JOME are 250.4 °C, 292.1 °C, and 266.5 °C, respectively. The ignition index for the B-20 blend is 73.73% more than that of diesel. The combustion index for the B20 blend is 37.81% higher than diesel. The B20 blend exhibits high enthalpy, better thermal stability, and a reduced peak temperature of combustion with an improved combustion index and intensity of combustion nearly comparable to diesel.

Keywords: biodiesel; combustion; thermal behavior analysis; simulation; TGA; DSC; vegetable oil; diesel engine performance

1. Introduction

The world is experiencing a shortage of fossil fuels and environmental degradation currently. Fossil fuel consumption leads to a reduction in underground carbon capacity. There is a need for us to develop an alternative fuel that can satisfy our day-to-day needs. Fuels derived from plants, biowaste, and animal waste are promising sources of energy [1]. Some of the biofuels can be used directly; however, some need improvement of their properties [2]. As biofuels may be of different origins, the properties vary from one fuel to another [3]. Biofuels can be blended with fossil fuels and can be used for various applications. When blended, each blend exhibits different properties. The majority of researchers extensively work on utilizing biofuels and their blends for engine applications [2,4–13]. The physiochemical properties have been evaluated by most researchers; hence, there is a need to evaluate the transport properties and the combustion phenomena. Knowledge of the thermodynamic properties also plays a vital role, but is rarely found in the literature. Thermal behavior analysis of biofuels and their blend is a new topic where attention is needed [7–9]. Hence, there is enough scope to analyze the thermal behavior of biofuels.

Ethyl esters and methyl esters have different structural effects on combustion phenomena. The C-O bond breaks in methyl esters, resulting in the formation of CH3 or CH3O radicals [14]. Through a six-member pericyclic transition state and a single-molecule elimination process, ethyl esters break down and release C2H4 [9]. Different degrees of unsaturation in fatty acids (which have a long chain of 8 to 24 carbon atoms) affect the oil and biodiesels' physical characteristics. Vegetable oils typically possess 95 percent triglycerides, 0.2% diglycerides, and 3% to 5% monoglycerides. The glycerin molecule is connected to fatty acids. Free fatty acids in vegetable oils (<3%) cause acidity [15,16]. A high level of unsaturated fatty acids reduces the fuel quality [17,18]. Unsaturated fatty acids such as oleic 18:1 and linoleic 18:2, which reduce fuel quality, are less stable than saturated fatty acids such as palmitic 16:0 and stearic 18:0 [15,16,19].

Stability is the major concern for the use of biodiesel as an engine fuel. Poor oxidation and thermal stability result in gum formation, leading to the problem of long storage [20–22]. Being highly susceptible to auto-oxidation process is the major concern for biofuel producers [23–25].

Research work carried out so far has described the evaporation and combustion mechanism of vegetable oils under different conditions of temperature and pressure. Heating and dilation take place before fuel vaporization when they are introduced in the diesel engine. To analyze this transient phase, knowledge of the transport properties, oxidation stability, and thermal stability is required, which are rarely available in the literature. The complexity of the thermal decomposition and kinetics of vegetable oils is due to complex series and parallel reactions. To address the combustion characteristics of biofuels, basic science related to kinematics and TG-DSC curves and their interpretations is applied. The types of methods to understand the combustion phenomena of biodiesels is important. The majority of the researchers have not used TG-DSC curves to analyze the combustion behavior. The significance of this review article highlights the importance of kinematics, as well as TG-DSC curves in order to understand the combustion behavior prior to testing. Efforts are summarized to bring clarity for researchers in the field of combustion studies by using thermal analysis methods. TGA and DSC studies will help to evaluate the combustion behavior and improve the storage conditions. Furthermore, these studies also help optimize the fuel blends prior to engine testing, thereby minimizing the engine bench tests. In the present article, an attempt is made to summarize the results of some research related to the kinetics of combustion, the effect of transport properties on combustion, thermal stability, oxidation stability, combustion characteristics, and combustion simulations. A case study is presented related to similar studies performed by a few researchers on thermal analysis. Diesel, JOME, and its B-20 blend are considered for the study. Peak combustion temperature, enthalpy, onset–offset temperature, stability, ignition, and burnout temperature are reported. The derivative thermogravitometry (DTG) curve is utilized, and the combustion index (S) and intensity of combustion (H_f) are evaluated.

2. Kinetics of Biodiesel Combustion

Table 1 summarizes the review of the few articles related to the kinetics of combustion. The effects of the fatty acid methyl ester composition, biodiesel purification process, and ethyl and methyl esters' combustion phenomena are discussed below.

Table 1. A summary of articles related to the kinetics of combustion.

Author(s)	Investigation	Fuel(s)/FAME	Findings
Abiola et al. (2013) [26]	Effect of fuel properties (such as boiling point, Cetane number, and oxygen content on the spray	Palm oil biodiesel and diesel	High boiling point of palm biodiesel produces high burning phase length; high Cetane number of flame; high Cetane number leads to shorter ignition delay
Ronghong Lin et al. (2013) [27]	Mechanism and kinetic decomposition of the biodiesel	Palm oil biodiesel	Stable up to 275 °C; further decomposition stages isomerization, polymerization, and pyrolysis reactions occur
Yan Luo et al. (2010) [28]	Effect of thermal cracking process to overcome cold flow and stability phenomena of biodiesel	Soy methyl ester and canola methyl ester	FAME of C24-C16 was reduced to low-molecular-weight hydrocarbons; decrease in cloud and pour point and thermal stability improved
Shin et al. (2011) [29]	Thermal decomposition of FAMEs from 325–420 °C with a pressure of 23MPa	Canole methyl ester	FAME is saturated or short chain length. then it has better thermal stability in supercritical methanol process
Osmont et al. (2010) [30]	Thermochemical data used for modelling biodiesel thermal decomposition.	1-, 2-, 3-, and 5-saturated alkyl radicals, monounsaturated 1-alkyl radicals	FAMEs via C-H, C-C, and C-O bond breakings are important to analyze combustion chemistry
Kent Hoekman et al. (2012) [31]	Reviewed 12 biodiesels' fatty acid profiles	Tallow, coconut, safflower, soya, sunflower, corn, etc.	Tallow and coconut exhibit high amounts of saturated fatty acids, whereas safflower, soy, sunflower, and corn have high unsaturated fatty acids
Sara Pinzi et al. (2013) [32]	Effect of biodiesel chemical structure on combustion and emissions		Unsaturated FAMEs were directly related to NOx emission; FAME with lowest carbon number gives low NOx emission, and high-carbon-number FAME gives high NOx emission; short and saturated FAMEs are preferred for biodiesel
Coniglio et al. (2013) [33]	Review article on thermophysical and thermodynamic properties of biofuels	Feed stock selection to find the thermodynamic properties	Better understanding of fuel properties is essential for the design procedure and combustion
Anitescu and Bruno (2013) [34]	Reviewed the combustion process of ethyl and methyl esters	Chemkin	Synergy between feedstock, its conversion, and combustion phenomena
Cordeiro et al. (2016) [35]	Effect of purification process on the stability	Jatropha biodiesel	Chemically purified wet method using anhydrous sodium sulphate and vacuum drying showed better thermal stability compared to dry method (purification with adsorbent magnesium silicate)
Goodrum (2002) [36]	Volatility and boiling points of different biodiesels using TGA	Canola oil, soybean oil, rapeseed oil, and tallow oil biodiesels	Boiling points from methyl to ethyl esters differ by 5 °C, respectively
Knothe (2005) [37]	Evaluated the properties of various fatty esters	Caprylic, capric, lauric, myristic, and palmitic ethyl and methyl esters	Chain length, degree of unsaturation, and branching of the chain are the important parameters
Lai et al. (2011) [38]	Review article on chemical kinetics modelling for biodiesel	Methyl butanoate was considered followed by isomers and unsaturated compounds	Kinetic modelling has the capacity to predict the early formation of CO_2 from methyl ester combustion; decrease in soot and increase in NOx emission

Table 1. *Cont.*

Author(s)	Investigation	Fuel(s)/FAME	Findings
Hoinghaus et al. (2010) [39]	Review article on combustion chemistry	Biodiesel to ethanol	Decomposition, oxidation mechanism, and formation of emissions; understanding chemical reaction network is a first step to analyze the combustion and emission
Li et al. (2019) [40]	Developed neural network model and compared with shock tube experiments	Surrogated fuels were considered (methyl decanoate, n-hexadecane, methyl trans-3-hexenoate, and 1, 4-hexadiene)	The behavior of large methyl esters of surrogated fuels was successfully analyzed; helped to analyze the ignition delay at various equivalence ratios and predicted activation energy at various levels
Liu et al. (2016) [41]	Directed relation graph error propagation and sensitivity analysis (DRGEPSA); analysis model was used with isomer lumping; 5025 species and 20,163 reactions	Methyl decenoate, methyl-5-decenoate, n-decane, and methyl linoleate	Developed skeletal mechanism is appropriate to predict ignition behavior, combustion characteristics, and NO_x emission
Wang et al. (2014) [42]	Ignition delay time measurement by performing reflected shock tube experiment	Methyl esters of soybean oil and animal fats consisting of methyl palmitate, methyl stearate, methyl oleate, and methyl linoleate	Ignition delay time was similar for all 4 methyl esters fuels, irrespective of their variation in organic structure
Saggesse et al. (2013) [43]	Lumped approach model for kinetic modelling (to analyze pyrolysis and oxidation behavior) with 420 species and 13,000 reactions	Rapeseed and soyabean methyl esters	Methyl palmitate and methyl stearate combustion behavior is similar to methyl decanoate; large unsaturated methyl esters are less reactive at low and intermediate temperatures
Westbrook et al. (2012) [44]	Used detailed kinetic model for simulating the combustion behavior; effect of C=C bonds on combustion behavior was analyzed	Single-component methyl esters, including methyl stearate, methyl oleate, methyl linoleate, methyl linoleate, and methyl palmitate	C=C bond is the key factor for Cetane number and ignition parameters; in the long chain hydrocarbons, more C=C leads to the reduction of the Cetane number; reduction in low temperature reactivity is directly proportional to the number of C=C bonds in each fuel
Zettarvall et al. (2017) [45]	Developed a skeletal chemical kinetics mechanism for LES involving 66 irreversible reactions between 23 species	Ethylene–air	Mechanism exhibits better performance with reduced computational time and numerical stability
Zettarvall et al. (2020) [46]	Developed new reduced chemical kinetics reaction mechanism for kerosene–air combustion with 30 species and 77 irreversible reactions	Kerosene–air	Developed kinetic mechanism presents good agreement with low computational cost, making it appropriate for combustion analysis using computational fluid dynamics (CFD)

The above literature concludes that the fatty acid methyl ester (FAME) proportion plays a vital role in the kinetics of biodiesel. Unsaturated and saturated fatty acids' proportions are very crucial for predicting the performance and emission parameters. C-H, C-C, and C-O bonds' breaking is important to study the combustion chemistry, whereas more C=C double bonds leads to a reduced Cetane number and ignition delay. The properties of biodiesels made from ethyl and methyl esters will differ significantly. Various researchers attempted to develop detailed kinetics models for analyzing the combustion chemistry. The developed models were compared with experimental results.

3. Transport Properties' Evaluation

Several investigators have reported on the effect of temperature and fatty acid composition on the thermal conductivity of different vegetable oils. Different vegetable oils (soyabean, sunflower, palm, copra, cotton, and jatropha) were considered in the temperature range of atmospheric to 2300 °C. The variation in the thermal conductivity values with the fatty acid

composition and temperature has been reported. The thermal conductivity value decreased from 0.167 W/m K at 20 °C to 0.137 W/m K at 230 °C [47]. Similar works on the measurement of the thermal conductivity of three distinct food oils, namely sunflower oil, corn oil, and olive oil, at temperatures of 25, 40, 60, and 80 degrees Celsius have been performed. A hot wire probe approach was used to obtain the measurements. The thermal conductivity of the oils decreased with temperature. At 25 °C, sunflower oil had a 0.168 W/m K thermal conductivity, while corn oil had a 0.152 W/m K thermal conductivity [48].

Fasina and Colley evaluated the viscosity and specific heat capacity of 12 different vegetable oils at various temperature from 35 to 180 °C using a rheometer and a differential scanning calorimeter. They reported exponentially decreasing trends for viscosity, while the specific heat capacity increased linearly [49]. Similarly, Simion et al. performed mathematical modelling for the measurement of the density and viscosity of different vegetable oils, namely olive, peanut, soyabean, almond, cotton, corn, sunflower, etc. [50]. Lima et al. examined different vegetable oils and their respective biodiesels for their phase equilibrium and thermal properties such as vapor pressure, boiling point, melting point, and critical properties, in addition to the properties of the organic compounds [51]. Miller et al. studied the heat transfer coefficient and viscosity for canola, corn, palm, and soyabean oil to analyze the frying phenomena. The frying time and oil temperatures majorly affected the viscosity. The oil degradation time affected the viscosity, whereas the heat transfer coefficient was not affected. Compared to all three oils, corn oil exhibited a good correlation to the viscosity and heat transfer coefficient [52].

Lopez et al. reported the thermal characterization of vegetable oils using photo acoustic techniques. Experiments were carried out for 13 vegetable oils for the evaluation of thermal diffusivity and effusivity; furthermore, using these data, the thermal conductivity and specific heat were determined [53].

Press and Pralat reported rheological behavior and thermal conductivity considering the shear effect by correlating the data with non-Newtonian fluids. Experiments were performed with three Newtonian liquids and 18 aqueous solutions at a concentration of 1000 to 5000 ppm with the temperature ranging from 299 to 315 K. The results showed that the increase in the concentration of the polymer in the aqueous solution reduced the thermal conductivity. The results were in good agreement with the developed mathematical models [54].

A few more research groups used different techniques to determine the thermal conductivity of liquids and gases. Codreanu et al. [55] presented an experimental setup that measures the thermal conductivity based on the transient hot wire methodology. Temperature was measured for a small interval time by using the RS 232. The platinum heater cum sensor of a 35 μm diameter was used with Teflon coating. The measured values were in good agreement with those published in the literature. Turgut et al. performed a new technique using the hot wire method to measure the thermal conductivity and diffusivity simultaneously. 3ω lock-in detection was used, where part of the signal yielded thermal conductivity and the phase signal yielded the thermal diffusivity. The relative measurements for thermal conductivity and diffusivity were found to be 0.1% and 0.3%, respectively [56]. Tavman and Turgut published a review article on various methods to determine the thermal conductivity of nanofluids. Most of the authors used the 3ω wire method to determine the thermal conductivity of SiO_2–water, TiO_2–water, and Al_2O_3–water nanofluids with different particle concentrations and various temperatures. The 3ω method contains a metallic wire, which acts simultaneously as the heater and sensor [57]. Tavman et al. [58] investigated the thermal conductivity and viscosity for deionized-water-based nanofluids with various volume fractions using the 3ω hot wire method. Initially, the experimentation was carried out for known fluids, and the results were validated with literature data. Then water-based TiO_2, SiO_2, and Al_2O_3 nanofluids were investigated, and the results were validated with the Einstein model.

Asseal et al. [59] presented the historical evolution of transient hot wire methods to determine transport properties. The article guides the reader through the design of the cell (heater dimensions, material, and thermal insulation) bridge circuit and different software used to monitor the temperature with respect to time. The required improvements in the method for determining transport properties for various state conditions were highlighted.

Paul et al. [60] presented a review article on various techniques to measure the thermal conductivity of nanofluids. Different techniques such as transient hot wire, thermal constant analyzer, steady-state parallel, cylindrical cell, temperature oscillation, and 3ω were explained in detail with the experimentation setup and analysis procedure. The authors concluded that the transient hot wire method is the more accurate one when compared to other methods.

Yusibani et al. [61] presented different methods of determining the thermal conductivity and thermal diffusivity of hydrogen gas by the 3ω method. They observed that the wire heat capacity also plays a vital role in determining the thermal conductivity, and the heater wire diameter should be less than 1 μm, neglecting the wire heat capacity. The heater wire of a nano-scale diameter is very useful for the accurate determination of thermal conductivity, neglecting the effect of convection and wire properties.

Assael and Wakeham [62] presented a review article on the importance of transport properties in the liquid and gaseous phase for engineering applications in the oil, chemical, biotechnology, and textile industries. The viscosity, thermal conductivity, and diffusion coefficient properties were discussed in detail. Various methods of determining the above properties with their advantages and disadvantages have been discussed in detail.

4. Thermogravimetry Analysis

Several investigators have reported on the thermal degradation of different biodiesels derived from vegetable oils.

The cold flow properties and oxidative stability of sesame oil methyl ester (SOME) were evaluated by Mujitab et al. [63]. The physiochemical properties of SOME indicated good cold flow properties due to a higher content of unsaturated FAs. Sesame methyl ester has shown good stability against rancidity. Shancita et al. studied the effect of the non-oxidation properties of pongamia and moringa biodiesels. An iron bar was dipped during the transesterification process in the biodiesel, which becomes oxidized, absorbing oxygen. Comparisons were made of the physicochemical properties, FAME composition, thermogravimetry, and IR analysis of neat biodiesel and oxidized biodiesel. The non-oxidation process improved the calorific value, oxidation stability, and Cetane number of pongamia biodiesel when compared to moringa biodiesel. TG-DSC studies also indicated improvements in storage stability and the thermal and oxidation process of the non-oxidated biodiesel [64].

Conceio et al. studied the thermal degradation of castor oil biodiesel by considering different temperatures from 150–210 °C in a synthetic air atmosphere with various exposure timings of 1 h, 12 h, 24 h, and 48 h. The percentage of mass loss, peak temperature, and enthalpy were studied as a function of temperature with a heating rate of 10 °C/min. Castor biodiesel presented stability up to 150 °C and degraded at a higher temperature, indicating the formation of intermediate compounds [65].

Yongbin Lai et al. conducted thermogravimetry experiments to investigate the volatility of palm oil, biodiesel, and its B-10 blend. A gas chromatography-mass spectrometer (GC-MS) was used to determine the chemical composition of the PME and -10 Petro diesel (-10PD). The volatility of the samples was measured using the volatility index. The palm biodiesel was made up of long-chain FAMEs: C14:0-C24:0, C16:1-C22:1, C18:2, and C18:3, and its B-10 blend was made up of long-chain alkanes: C8-C26. Palm oil biodiesel volatilization was stronger and faster, but it started at a higher temperature. PME and -10PD had volatilization start temperatures of 448.9 K and 361.7 K, respectively, and volatility indexes of 1.76×10^{-4} and 3.64×10^{-5} [66].

Santos et al. investigated the thermal stability and physiochemical properties of biodiesels derived from cotton, sunflower, and palm oil along with their B-10 blends. TG curve of the palm oil indicated a high initial temperature of decomposition and two mass loss steps, whereas one mass loss in the case of sunflower oil and cotton oil was observed. The high onset temperature of cotton oil biodiesel indicates high thermal stability when compared to palm and sunflower oil biodiesel. Blends exhibited a higher decomposition temperature [67].

K. Subramanian et al. studied the thermal degradation of sunflower, coconut, gingelly, and ground nut oils by simultaneous TGA-DTA experiments. The thermal and thermo-oxidative stabilities and decomposition enthalpies of refined and virgin oils in an air and nitrogen atmosphere were simultaneously analyzed to optimize their process, use, and storage conditions for stability and reusability. The oils were negligibly degraded below 200 °C [68].

Wnorowska et al. examined the effect of a fuel additive on different fuels to analyze the combustion profiles. Halloysite was used as a fuel additive, and they generated TG-DTG profiles for analyzing the combustion profile [69].

Bica et al. studied the thermal degradation of rapeseed biodiesel and interpreted TG-DTG and DTA thermograms for the B-10, B-20, B-40, and B-50 blends. They reported that the distillation interval was found to be higher for the biodiesel and its blends when compared to that of diesel. They also indicated the exothermic and endothermic behavior with stability [70].

Dwivedi and Sharma reported the oxidation and thermal stability of pongamia biodiesel with respect to its deterioration and long storage capacity. Oxidation stability, onset–offset temperatures, and variation of the activation energy were reported by considering the blends of pongamia biodiesel with varying proportions of the pyrogallol (PY) antioxidant from 100–500 ppm and iron metal contaminants of 0.5, 1, 1.5, and 2 mg/L. Studies revealed that the thermal degradation of all the samples of Pongamia biodiesel followed the first-order reaction. The addition of the PY antioxidant increased the induction period and activation energy, while the addition of iron metal contaminants decreased the induction period and activation energy [71].

Czarnocka et al. studied the degradation process of diesel fuel by considering two sets of diesel fuel named ONH-1 and ONH-2 ONH-1 containing 6.8–7.2 (v/v) of fatty acid methyl esters and ONH-2 being pure hydrocarbon. The first one, denoted as ONH-1, was kept in a small standard over-ground vessel with a capacity of 0.2 m^3, whereas the second one, denoted as ONH-2, was stored in a subterranean tank with a capacity of about 4 m^3 for a period of 12 months with different pre-conditions and time intervals, in accordance with the time interval. The authors concluded that ONH-2 oil stored in the subterranean tank degraded more slowly, because it was less exposed to the weather conditions [72].

Souza et al. reported on enzymatic synthesis of Jatropha oil methyl ester with ethanol in a solvent-free system and transesterification carried out in microwave irradiation. The fuel properties obtained with the above-mentioned technique were compared with the conventional heating method. The generated TG-DTG curves were compared with the standard ethyl ester [73].

Silva et al. studied the thermal stability of biodiesel derived from sunflower oil through a heterogeneous catalyst process. KNO_3/Al_2O_3 were considered as catalysts with a 2, 4, 6, and 8% weight percentage. The 4% KNO_3/Al_2O_3 catalyst showed better catalytic activity in the transesterification reaction of sunflower oil under the conditions adopted, having a conversion of 60% ethyl esters [74].

Farias et al. examined the thermal stability of biodiesel blends in 20% passion fruit, 20% castor oil biodiesel, and a 20% biodiesel blend of passion fruit and castor oil. The TG curve indicated a higher stability of the castor oil biodiesel when compared to passion fruit. The presence of oleic and linoleic acids in the passion fruit showed low thermal stability due to high oxidation. Blends of the passion fruit and castor oil biodiesel (1:1 proportions) indicated high thermal stability, whereas the high stability in 1:2 proportions was due to the ricinoleic acid content in castor oil [75].

Ayhan Demirbas studied the thermal degradation of sunflower seed oil during biodiesel production. The results revealed that, during the thermal degradation process, the double bonds of the unsaturated aliphatic carbon chains in the fatty acids underwent the degradation process first. Biodiesel oxidation results in hydroperoxides' formation. Unsaturated olefinic fatty acid oxidation occurs in multiple steps, forming numerous secondary oxidation products [76].

Todaka et al. studied the thermal behavior of biodiesels derived from rapeseed, coffee, and jatropha oils. Thermogravitometric experiments were conducted in an air and nitrogen atmosphere. A higher decomposition temperature was observed if higher chain alcohols were used during the transesterification process. Butanol-based biodiesels showed a higher thermal stability of 30 °C when compared to methanol-based biodiesels [77].

Peer et al. investigated the oxidation stability of biodiesel made up of Calophyllum inophyllum with its B-20 blend. The effect of pentanol with 10% and 15% on the fuel was also studied. The biodiesel showed an induction period of 8.47 h, while by adding 10% of pentanol, the induction period improved by 44.57% compared to the B-20 blend. The addition of 15% of pentanol reduced the induction period by 19.48% compared to the addition of 10% of pentanol [78].

Khurana and Agarwal studied the oxidation stability phenomena of biodiesels made up of karanja and neem oil with the addition of the pyrogallol (PY) antioxidant. Karanja, neem, and jatropha biodiesel exhibited onset temperatures of 148 and 153 °C, respectively. The addition of the antioxidant increased the stability. The results revealed that the jatropha biodiesel was thermally more stable compared to the karanja and neem biodiesel blends [79].

Dunn et al. investigated the oxidative reaction using pressurized-differential scanning calorimetry (P-DSC). Methyl linoleate, methyl oleate, and soybean oil fatty acid methyl esters were analyzed and compared with the thermogravimetric results. Methyl oleate represented the highest onset temperature during the DSC and P-DSC experimentation. The onset temperature for the soybean oil fatty acid methyl ester could be improved by the addition of antioxidants [80].

Agarwal et al. studied the influence of antioxidants on the thermal stability of karanja, neem, and jatropha biodiesels using five antioxidants: 2,6-di-tert butyl-4-methyl phenol (BHT), 2-tert butyl-4-methoxy phenol (BHA), 2-tert butyl hydroquinone (TBHQ), 1,2,3 tri-hydroxy benzene (PY), and 3,4,5-tri hydroxy benzoic acid (PG). When compared to the karanja biodiesel, the jatropha biodiesel showed higher oxidation stability. The ASTM oxidation stability requirement was not met by the neem biodiesel [81].

Shameer et al. investigated the effect of the tert-butyl hydroquinone (TBHQ) antioxidant on Calophyllum inophyllum biodiesel to analyze the long-term storage stability and thermal stability. FTIR spectroscopy was used to study the oxidation stability. TBHQ with a 1000 ppm concentration was added to the biodiesel in a 1–5 weight concentration. B100A3 showed improved oxidation stability, thermal stability, and storage stability [82].

Mothe et al. investigated the optimal reaction conditions for the transesterification process of waste frying and fish oil with various reaction times, catalysts, and temperatures. The thermogravitometry results showed two steps of decomposition with onset temperatures of 180 °C and 280 °C. The DSC curve also predicted three endothermic events by confirming the decomposition of the biodiesel, oil waste, and inorganic waste [83].

Christensen and McCormick considered four sets of biodiesels, namely A, B, C, and D with their B5 and B20 blends for the stability (aging studies) with the addition of an antioxidant. The real-time experimentation was simulated to analyze the stability of one year for the biodiesel and three years for the blends. The results concluded that the B5 blends were stable, whereas the B20 blend was unstable if prepared from high polyunsaturated ester biodiesel with a 3 h induction time, but B20's stability satisfied the ASTM conditions; hence, blends varying from 5 to 20 can be considered as alternatives [84].

Freire et al. analyzed the thermal behavior of several oils and their biodiesels. Thermogravimetry (TG) and pressurized-differential scanning calorimetry (PDSC) experiments were performed to analyze the thermal behavior. The fuel samples were named as 2005/2006, 2006/2007, 2007/A, 2007/B oil, and biodiesel, respectively. The 2007/B and 2007/A biodiesels were thermally stable up to 203 °C and 108.9 °C, respectively. The 2005/2006 crop oil and biodiesel were thermally less stable compared to the others due to the high water content of the seeds [85].

Jose and Anand considered biodiesel blends of coconut and karanja with diesel (karanja, coconut biodiesel, 20% karanja and 80% coconut blend, 50% karanja and 50% coconut blend, 20% Karanja and 80% diesel, 50% karanja and 50% diesel) to analyze the effect of biodiesel composition on long-term storage. All the fuel samples were kept under different storage conditions for 10 months, and important physiochemical properties and compositions were evaluated at regular intervals of times. The results concluded that the karanja biodiesel exhibited a high rate of degradation compared to all the blends. Blending of karanja and coconut biodiesel exhibited reduced degradation upon long-term storage, and blending with diesel resulted in a high rate of degradation compared to the blends [86].

Macedo et al. analyzed the thermal behavior of oiticica oil and its biodiesel. Thermogravitometry studies were performed in air and nitrogen for thermal stability analysis. In the synthetic air atmosphere, the biodiesel possessed three stages of decomposition with mass losses of 12, 72, and 16%. In the nitrogen atmosphere, the biodiesel exhibited two stages of decomposition with mass losses of 13.5 and 86.5%. The results revealed that the oil and biodiesel were thermally stable up to 224 °C and 179 °C, respectively [87].

Rashed et al. presented a review article on biodiesel stability by reviewing various concepts such as oxidation, thermal stability, and storage stability. The mechanism of decomposition, the effect of different parameters on the stability, stability measurements, and the methods to improve the stability were discussed. The acid value, induction period, iodine value, peroxide value, viscosity, and density were the major parameters that affected the stability. Infrared spectroscopy is an effective and easy method for oxidation stability analysis. TGA/DTA and the Rancimat test are efficient methods to determine thermal stability. Pyrogallol (PY), propyl gallate (PG), and Tert-butylhydroquinone (TBHQ) are the efficient stability improvers. Out of all three, PG is the best one and has decreased NOx emissions. Aluminum is the best material for biodiesel storage purposes [88].

Perez et al. studied different pyrolysis oil and bio-diesel mix ratios on oxidation stability. The bio-oils were produced utilizing the semi-continuous auger pyrolysis of pine pellets and the batch pyrolysis of pine chips. The addition of bio-oil increased the oxidation stability by altering the crystallization behavior of the unsaturated molecules and increasing the onset temperature. This is mainly due to the presence of the phenol groups [89].

Various researchers have performed TG analysis in various fuels. It helps to analyze the thermal stability of the fuel. TG results can be correlated with the fatty acid methyl esters' proportion to understand the different decomposition ranges. Few researchers have used additives with various proportions to compare the improvement of the thermal stability. The first derivative of TG, i.e., the DTG curve, can be analyzed in detail to evaluate the combustion indexes. Different kinetic models can be used such as the Arrhenius model to evaluate the activation energy for various conversion rates.

5. Differential Scanning Calorimetry Analysis

Table 2 depicts the summary of the research articles related to the study of the volatility parameters, oxidation stability, and cold flow parameters.

Table 2. A summary of articles related to DSC analysis.

Author(s)	Investigation	Fuel(s)/FAME	Findings
Nair et al. (2019) [90]	TGA-DSC, GC, FTIR	Algae biodiesel	Higher algae biodiesel contains high oleic and linoleic acid, and biodiesel is stable up to 360 °C
Samaraae et al. (2017) [91]	Fuel characterization using FTIR and DSC	Safflower biodiesel and its blends	Biodiesel can be blended with diesel and butanol as ternary blend up to 20%
Leonardo et al. (2016) [92]	Volatility parameters studied using DSC—open and closed pan	Diesel S10	When using open pans, boiling occurs at a lower temperature due to the dragging effect of the purge gas
Stenseng et al. (2001) [93]	TGA and DSC for estimating the pyrolysis, char reactivity, and ash melting behavior	Coal	TGA and DSC scan be successfully applied for combustion research
Malvis et al. (2019) [94]	DSC used to evaluate fatty acid composition of four extra virgin oils with different heating rates	Virgin oils	Higher heating temperature leads to high onset oxidation temperature
Robertis et al. (2011) [95]	Esters' analysis using DSC	Soya biodiesel and animal feedstock	Critical temperatures of esters can be analyzed successfully by using DSC
Melo at al. (2014) [96]	Pressurized-DSC for evaluating the oxidation stability	Andiroba, babassu, sesame, oiticica, jatropha, and grape oil	Babassu, jatropha, and andiroba are potentially stable for biodiesel production
Ramalho et al. (2011) [97]	DSC, TGA, and DTA in different atmospheres	Poultry fat and its ethyl (BEF) and methyl (BMF) biodiesels	Four exothermic reactions were observed in synthetic air and a single endothermic reaction in a nitrogen atmosphere; the TG-DTG curve exhibits two phases of decomposition for both biodiesels in the air and nitrogen atmosphere
Santos et al.(2018) [98]	Thermal and oxidative behavior using DSC and TGA	Muruci oil	Oil is stable up to 200 °C with the exothermic peak at 250 °C; oxidative induction time for the sample found to be 20.85 h
Donos et al. (2020) [99]	DSC studies were carried out for oxidation stability analysis	Grapeseed oil fatty acid ethyl ester and methyl esters	Grapeseed oil ethyl ester satisfies the biodiesel criteria, whereas additives are required for grapeseed oil methyl ester
Borugadda and Goud (2013) [100]	DSC studies to examine the thermo-oxidative stability and cold flow parameters	Waste cooking oil (WCO) and castor oil (CO)	WCO found to be thermally more stable, but exhibits less oxidation stability compared to CO; castor oil shows improved pour point and cold point over WCO
Leonardo et al. (2019) [101]	DSC studies and carried out oxidation studies	Soyabean biodiesel and its blends	Addition of biodiesel to diesel modifies the vaporization profile of the fuel, as well as increases the onset temperature

DSC studies help to evaluate the oxidative stability and cold flow parameters of the fuels. The DSC curve can be interpreted to know the type of chemical reaction, either exothermic or endothermic. The heat flow rate, enthalpy, and reaction range can be determined from the DSC curve. Various researchers have investigated the vaporization profile and oxidation behavior of biodiesels and their blends with and without additives to determine the improvement of the parameters. The majority of the researchers reported on the DSC curve, showing a two-phase decomposition for biodiesel and a single phase of decomposition for its blends (up to 20%).

6. Combustion Characterization Using TG Curve

Alaba et al. investigated biodiesel production kinetics using mesoporous ZSM-5 zeolites (0.3mesoZBio and 0.4meso ZBio) and regular ZSM-5 zeolites (Z-Bio). Different

heating rates of 10, 15, and 20 per minute were used in the pyrolysis tests. Four distinct kinetic models were used to calculate the reaction order, activation energy (EA), and frequency factor (A). In comparison to 0.3 mesoZBio and 0.4 mesoZBio, ZBio had the highest EA (86.53 kJ mol^{-1}) (84.92 and 83.26 kJ mol^{-1}, respectively). ZBio was found to be the most stable [102].

Morais studied the thermodynamic parameters of solid biofuel from orange peel. Thermal analysis of the dried peel revealed three mass loss events. The material's thermal stability improved as the pyrolysis temperature rose. The Ozawa–Flynn–Wall method was used to determine thermodynamic parameters such as enthalpy (H°), Gibbs free energy (G°), entropy (S°), and the pre-exponential factor (A) [103].

Yongbin Lai et al. investigated the combustion characteristics of palm oil and rapeseed oil biodiesel. The chemical composition was determined using GC-MS. In the TG-DSC simultaneous analyzer, combustion tests were carried out. PME and RME had a 35.86 and 14.69 wt% saturated FAME concentration, respectively. The combustion feature was linked to the saturated FAME. PME had superior combustion characteristics [104].

In Andrade et al., buriti oil biodiesel and its numerous blends with diesel were considered (B2, B5, B10, B201, B50, and B100). Thermal analyses of the blends were carried out at a rate of 10 °C per minute in the 30–600 °C range. The Coats–Redfern equation was used to calculate the kinetic parameters such as the activation energy (Ea), pre-exponential factor (A), Gibbs energy (G), enthalpy (H), and entropy (S) of activation. The biodiesel blends reduced the heat of combustion [105].

Hui Li et al. considered peanut oil and its biodiesel and investigated the thermal degradation of the biodiesel and its feedstock through TGA in combination with FTIR. Experiments were carried out under different heating rates of 5, 10, 15, and 20 K min^{-1} in the temperature range of 298 to 873 K. Peanut biodiesel and peanut oil exhibited only one weight loss stage during the whole thermal degradation process, and the onset and endset temperatures were lower than those of peanut oil. The POB activation energies (Ea) increased from 43.22 to 56.22 kJ mol^{-1}, whereas that of PO increased from 86.24 to 157.73 kJ mol^{-1}. A similar trend was observed for the enthalpy [106].

Volli and Purkait examined the thermo-chemical behavior of mustard, soybean, olive, and karanja oils. TG-DTG experiments were conducted in a nitrogen atmosphere up to 600 °C with heating rates of 10, 20, 30, 50, and 100 °C/min. They observed a single stage of decomposition. High activation energy was noticed in karanja followed by soybean, mustard, and olive oils [107].

Imdadul et al. studied the effect of ignition improvers on thermal stability and engine performance. The authors considered the blend of diesel–biodiesel and pentanol with 2-ethylhexyl nitrate (EHN) as an additive at a 1000 and 2000 ppm proportion. The results revealed that the addition of the additives improved the Cetane number and thermal stability. BSFC, NO, and smoke were reduced [108].

Wang et al. studied the oxidation characteristics of methyl and ethyl esters having a carbon number less than six. Methyl formate, methyl acetate, methyl propionate, methyl butanoate, ethyl formate, ethyl acetate, and ethyl propionate were considered for the study with atmospheric pressure and elevated reactant temperature conditions to determine the laminar flame speeds. The experimental results were compared with the simulated results. Overall, the work carried out highlights the importance of alkyl-ester combustion chemistry in deriving the rate constants [109].

Arruda et al. studied the thermal behavior of sesame oil and its biodiesel obtained from methyl and ethyl alcohol by using gas chromatography (CG/MS), NMR, and thermo-gravitometry. Biodiesel showed a single-step decomposition, whereas sesame oil showed three steps of decomposition. The average value of the kinetic energy was found to be 67.54 and 66.74 KJ mol^{-1} for the methyl and ethyl biodiesel, respectively [110].

Kok et al. (1993) [111] conducted an extensive review on the application of the thermal analysis method for analyzing pyrolysis and combustion behavior. Lignite, bituminous coal, anthracite, oil shales, and crude oil were reviewed.

Avila and Sodre investigated the physiochemical properties and thermal behavior of fodder radish crude oil and its biodiesel. The biodiesel produced from fodder radish oil met the specific criteria for biodiesel, except the acid number. The TG-DTG result showed a single-step volatilization of methyl esters, which is favorable for the combustion process [112].

Borsato et al. studied the influence of temperature on the oxidation stability of soya biodiesel with the addition of an antioxidant. The thermodynamic properties such as the Gibbs free energy and enthalpy for the biodiesel were evaluated. The results concluded that the biodiesel had low oxidation resistance, but the addition of a synthetic antioxidant improved the oxidation stability. The centroid mixture design was found to be suitable for the optimal selection of the antioxidant [113].

Andrade et al. evaluated the heat of combustion for soya biodiesel and its blends. The authors concluded that the addition of biofuels for diesel reduced the heat of combustion due to the presence of an organic chain. C-O and C-C bonds will act as resistance to the heat flow. The authors concluded that the heat of combustion of the biodiesel was nearly 17% less than the diesel [114].

Arudda et al. considered waste cooking oil and moringa biodiesel with diesel blends for thermogravitometry studies to determine and analyze the storage conditions and activation energy. The results concluded that the moringa oil biodiesel was more stable than the waste cooking oil biodiesel. The addition of the moringa biodiesel to the waste cooking oil biodiesel did not affect the stability. The average value of the kinetic energy for the moringa biodiesel and the waste cooking oil biodiesel was found to be 53 and 74 kJ/mol, respectively [115].

Conconi and Crnkovic analyzed the thermal behavior of farnesene biodiesel, soya biodiesel, and diesel with their blends 20F80D and 20F50D30B. Thermogravitometry studies were carried out to analyze the thermal behavior and kinetics study. The results revealed that the DTG profile for pure biodiesels occurred in a narrow range, whereas, for diesel, a broader decomposition range could be observed. Famesane exhibited less activation energy compared to soya biodiesel, subsequently showing improved combustion. The presence of diesel in the blends lowered activation energy initially and, accordingly, affected the blends' performance at the end stage of combustion. The activation energy for the fuels was found to be 82, 86, and 96 kJ/mol for the farnesene, diesel, and soya biodiesel, respectively [116].

Crnkovic et al. determined the activation energy for three different fuel samples, namely A, B, and C. Thermogravitometry and differential thermal analysis tests were performed for different heating rates from room temperature to 600 °C. During the interpretation, the authors analyzed three different stages of decomposition, low-temperature oxidation (LTO), fuel deposition (FD), and high-temperature oxidation (HTO). The median value of the activation energy was considered for a conversion rate ranging from 1% to 90%. The activation energy was found to be 43.8, 57.2, and 61.8 kJ/mol for fuel samples A, B, and C, respectively [117].

Jain and Sharma analyzed the thermals stability and activation energy of jatropha biodiesel. The thermogravitometry results showed that the thermal degradation followed the first-order reaction. Direct Arrhenius plots were used to determine the activation energy. Different antioxidants were considered for the study, and the results concluded that the addition of the antioxidants affected the onset temperature and activation energy. Compared to all four antioxidants of propyl galate (PG), tert-butyl hydroquinone (TBHQ), butylated hydroxytoluene (BHT), and butylated hydroxyanisole (BHA), propyl galate optimized them the most [118].

Mortari et al. evaluated the ignition behavior and kinetic parameters of sugar cane bagasse, coal, and their blends. Thermogravitometry studies were carried out, and the results were analyzed. The ignition temperatures for the bagasse, coal, and their blend were found to be 256 °C, 427 °C, and 275 °C, respectively. The activation energy was studied for the combustion and pyrolysis mechanism in an air and nitrogen atmosphere. The activation energy was found to be 170.8 and 277.8 kJ/mol in the synthetic air atmosphere, whereas in the nitrogen atmosphere, it was found to be 185 and 82.1 kJ/mol [119].

Xing et al. studied the combustion characteristics of waste plastics and a semicoke mixture by using the thermogravitometry method from room temperature to 1173 K with various heating rates. The kinetic parameters were calculated by using the n-order rate model of a double parallel reaction. The results revealed that the combustion process for waste plastic was found to have mixed combustion phenomena, whereas for semicoke combustion, the phenomena could be divided into two stages, i.e., into the volatile combustion stage and the fixed carbon combustion stage. As the heating rate increased, the mass loss peak moved to the high-temperature zone. The maximum value of the combustion index (S) and flame index (C) was found to be for a heating rate of 20 K/min [120].

Song et al. evaluated the combustion behavior of lignite coal and coal gangue with their blend ranging from 25–75 wt% by utilizing the thermogravitometry method with an ambient temperature of 1000 °C. Sixty percent of the coal gangue showed optimized combustion parameters. The carbon number of the coal played a vital role in combustion: a higher carbon number indicates a higher ignition temperature. Blending of the coal with the coal gangue showed better combustion behavior compared to coal alone [121].

Kok and Topa investigated the combustion and pyrolysis behavior of diesel and canola oil by performing differential scanning calorimetry (DSC) and thermogravimetry (TG-DTG) experiments at different heating rates. The peak temperature of the reaction shifted to the higher side as the heating rate of the reaction increased. The DSC combustion curve implied that the reactions of pure samples were exothermic in nature. A kinetic study showed that an increase in the heating rate resulted in increased activation energy [122].

Liu et al. studied the pyrolysis and kinetic behavior of wheat stalk bio-oil by performing thermogravimetry experiments. The results concluded that pyrolysis occurred in three phases: volatilization of light fractions, decomposition of heavy fractions, followed by char combustion. The activation energy during the volatilized phase was higher than the decomposition phase, as both phases exhibited first- and second-order reactions [123].

Soto et al. evaluated the behavior of biofuel and fossil fuel by performing TG and differential thermal analysis (DTA) experiments. Engine tests were performed for pure biodiesel and diesel with their B20 and B50 blends. Two and three phases of decomposition were observed for diesel and biodiesel with ignition temperatures of 250 °C and 300 °C, respectively. Activation energy ranged from (48.5–61.0) kJ mol^{-1} and (58.6–55.0) kJ mol^{-1}, respectively. During the initial phase of combustion, diesel exhibited lower activation energy with the ignition temperature compared to the biodiesel, and the opposite behavior was observed during the final stage of combustion. Blending diesel with biofuel was shown to be the best option [124].

Ninduangdee et al. analyzed the combustion behavior of palm oil residues and kernel shell by performing thermogravimetry experiments. The experiments were performed from 30 °C to 900 °C with four different heating rates: 10–40 °C/min. The palm oil exhibited higher thermal and combustion reactivity compared to the kernel shell due to a lower ignition and burnout temperature and less activation energy [125].

Wang et al. carried out a thermal and kinetic analysis on bio-oil derived from swine manure (crude glycerol) by performing thermogravimetry experiments. Three phases of decomposition were observed where the maximum compound decomposition occurred in the range of 330–370 °C. Kinetic studied were carried out by using the Coats–Redfern method. Four models including 12 alpha functions were tested and fit with the experimental results. Out of the four models, the diffusion model was found to be better for the combustion process [126]. The majority of the researchers in the early stage used the TG-DTG curve to evaluate the combustion parameters for different types of coals. Few researchers have adopted the same procedure to analyze similar parameters for biodiesels. Ignition parameters such is ignition temperature, burnout temperature, and maximum rate of decomposition have been analyzed. Furthermore, with the help of the DTG curve, the ignition index, burnout index, combustion index, and intensity of combustion have been evaluated. Different kinetic models such as the Coats–Redfern, Ozawa–Flynn–Wall, and Arrhenius models have been used by various researchers to analyze the kinetics of combustion.

7. Combustion Simulation

Combustion simulations have been performed by several researchers utilizing different commercial software packages (see Table 3).

Table 3. A summary of articles related to combustion simulation.

Author(s)	Tool Used	Studied Parameters	Findings
Jafarmadar and Zehni (2012) [127]	AVL-FIRE code CFD	High-speed diesel engine combustion phenomena	Reduced computational time was observed for the developed code with a coarse mesh
Raj et al. (2012) [128]	Extended Coherent Flame Model for 3 zones (ECFM-3Z)	Effect of swirl ratio on a constant speed diesel engine	Variation of the swirl ratio from 1.4 to 4.1 affects soot emission and NOx emission
Baratta et al. (2020) [129]	Converge CFD model	Combustion phenomena with different EGR rates and hydrogen doping conditions	Results obtained by the Converged CFD tool were closely comparable with the experiments
Costa et al. (2018) [130]	Reduced chemical kinetics coupled with turbulence and through a turbulent species transport approach with detailed kinetics	Combustion efficiency studies on premixed syngas and biodiesel as pilot injection	Increasing the percentage of syngas decreased the combustion efficiency, whereas the exhaust gas temperature and thermal efficiency increased; the reduced chemical kinetics model gave an improved solution over a detailed kinetics model
Maghbouli et al. (2013) [131]	3D-CFD/chemical kinetics framework model	Pressure, ignition delay, and heat release rate	Simulation results were in good agreement with the experiments
Vijayshree and V Ganesan (2018) [132]	Overview about the application of CFD for analyzing and designing IC engines	1. Different valve lift condition; 2. multi-cylinder inlet manifold for different valve lift conditions of 25%, 50%, and 100%; 3. steady flow analysis on the six-cylinder V-Engine	CFD can be used as a powerful tool for designing IC engines and to analyze the combustion process

Thermogravitometry and differential scanning calorimetry are used to investigate the thermal behavior of biodiesels and their blends. Traditional engine testing is a time-consuming process and requires a huge quantity of fuel. This testing process provides performance parameters only. It is possible through TG-DSC to assess the optimal fuel blend's combustion performance. In addition, TG-DSC curves indicate the oxidation behavior of biodiesels and their blends, the heat flow parameters, and the thermal stability for storage conditions.

8. Case Study

TGA and DSC experimentation was carried out in an air atmosphere with a heating rate of 10 °C/min in a calorimeter, model NETZSCH STA 449F3, made by NETZSCH group, Germany. The generated DSC and TG curves were analyzed for the peak combustion temperature, enthalpy, onset–offset temperature, stability, ignition, and burnout temperature. The DTG curve was utilized, and the combustion index (S) and intensity of combustion (Hf) were evaluated. The DSC combustion curve and the TG-DTG curve are shown in Figures 1 and 2. Furthermore, the TG-DTG curve was analyzed in detail to determine the combustion indexes. The results of the recent published work can be found in [133–136]. The Taguchi design of experiments is also one of the competitive tool used to

reduce the number of bench experiments. Taguchi's L9 orthogonal array can be used to obtain the optimal solution [137,138]. Figures 1 and 2 depict the DSC curve for JOME and its B-20 blend, and Figures 3–5 represent the TG-DTG curve for diesel, JOME, and its B-20. Figure 6 depicts the stages of combustion, which can be analyzed in detail to determine the combustion indexes.
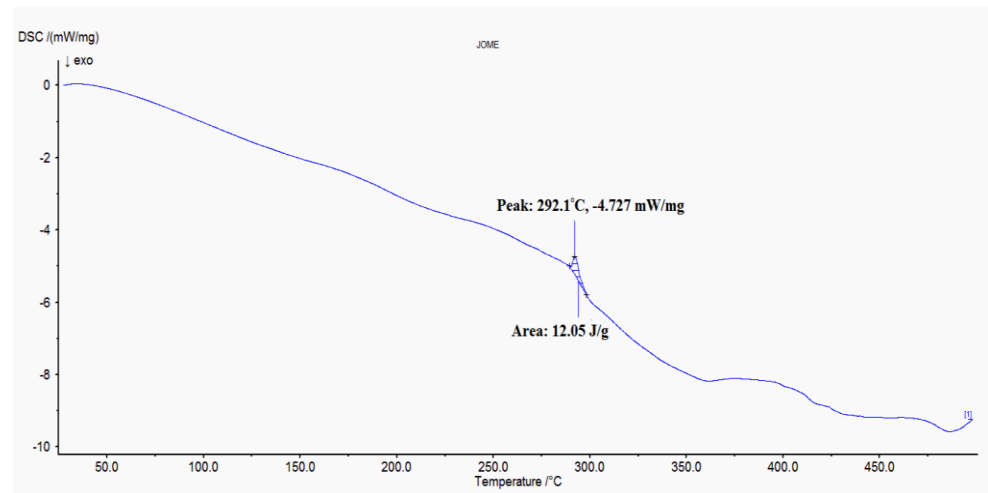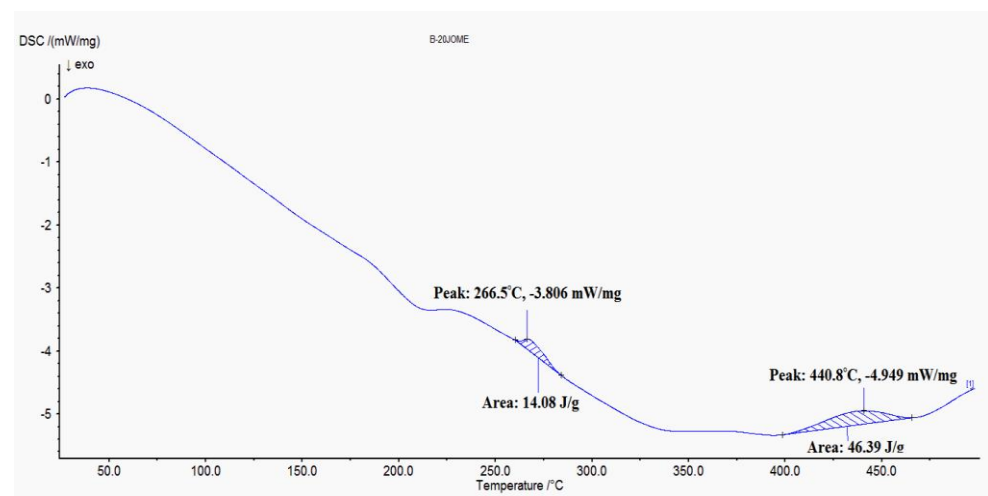

Figure 1. DSC combustion curve for JOME.
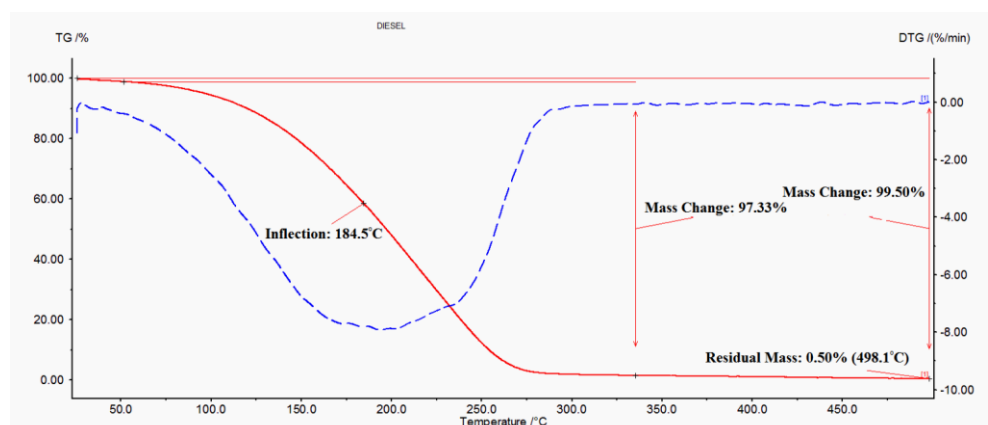

Figure 2. DSC combustion curve for B20 JOME.

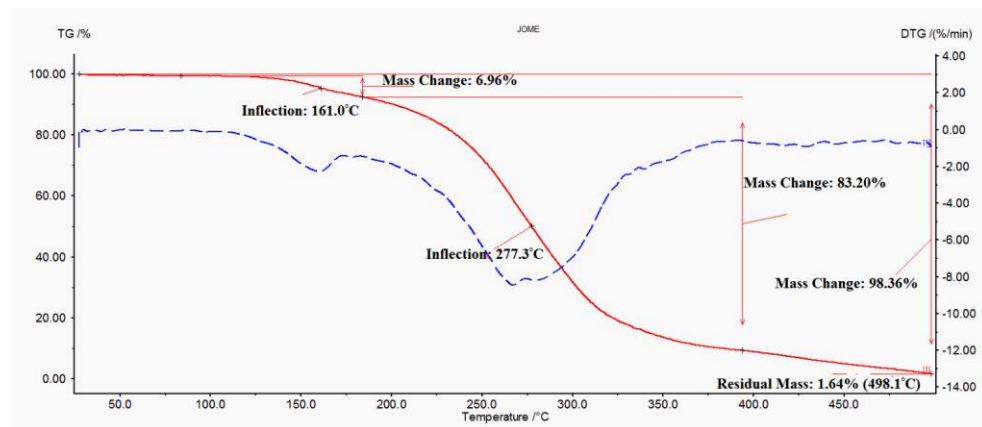**Figure 3.** TG-DTG curve for diesel.

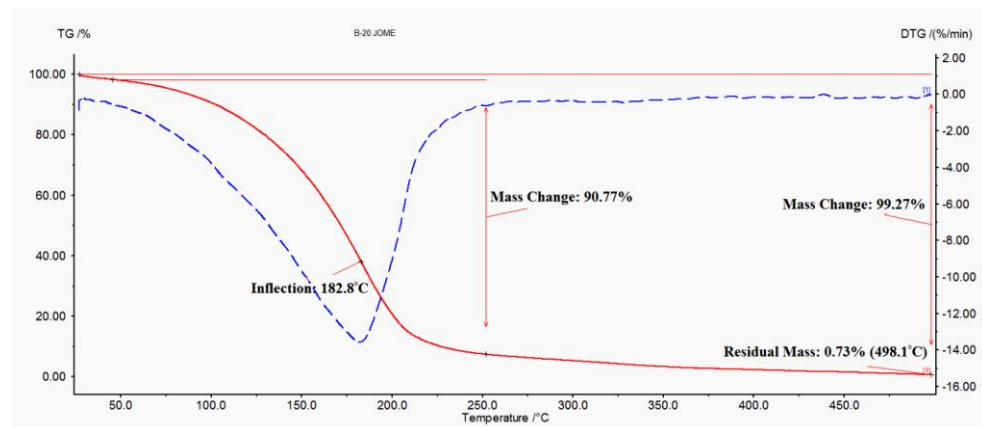**Figure 4.** TG-DTG curve for JOME.

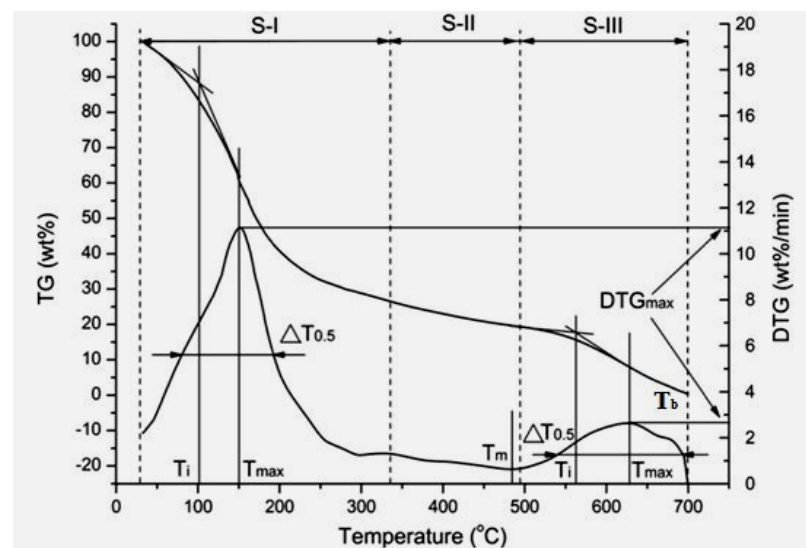**Figure 5.** TG-DTG curve for B20 JOME.

Figure 6. Combustion stages from the TG-DTG curve [120].

Diesel molecules have different lengths, behaviors, and properties. Figures 1 and 2 represent the degradation curves for diesel, JOME, and B-20 JOME. Diesel fuel starts to degrade around 40 °C to 498 °C with a time span of 47.26 min, and the remaining mass represents soot particles. Napthenes, paraffins, olefins, and aromatic compounds present in the diesel with C_{12}–C_{18} decompose in the range of 118.25 °C to 255.25 °C. JOME contains

linoleic acid, oleic acid, and palmitic acid, which decompose at 240 °C, 272 °C, and 360 °C, respectively. Linolenic, stearic, and behenic fatty acids starts to decompose above 300 °C. Tables 4 and 5 depict the parameters analyzed by DSC and TGA.

Table 4. Heat flow and enthalpy at peak temperature.

Sample	Reaction Region (°C)	Peak Temperature (°C)	Heat Flow (mW/mg)	Enthalpy (J/g)
Diesel	34-270	250.4	−1.851	130.4
JOME	43-435	292.1	−4.727	12.05
B20 JOME	63-465	266.5	−3.808	147.5

Table 5. Onset, offset, reaction region, maximum temperature, and weight loss biodiesels.

Sample	Onset Temperature, Te (°C)	Offset Temperature, To (°C)	Reaction Region (°C)	Decomposition Temperature, Tmax (°C)	Weight Loss (%) at 498.1 °C
Diesel	140	265	40–280	184.5	99.50
JOME	146	334	140–490	277.3	98.36
B20 JOME	130	230	40–430	182.8	99.27

The thermal degradation of JOME occurs in the following order: methyl esters evaporate initially, followed by decomposition of monoglycerides, diglycerides, and triglycerides; high carbon fatty acids finally carbonize. B-20 JOME decomposes in the range of 40 °C–390 °C, similar to diesel, with a higher offset temperature, meaning the molecules of JOME and diesel form a homogenous mixture at 20%. The oxygen content in the biodiesel acts as an agent for easier decomposition. The decomposition temperature increases with the increase in the biodiesel content. Tables 6 and 7 represent the combustion characteristics obtained by analyzing the TG-DTG curve.

Table 6. Ignition, burnout temperature, DTGmax, and Tmax of diesel, JOME, and B20 JOME.

Sample	Ignition Temperature (°C)	Burnout Temperature (°C)	DTG Max	Tmax Corres DTG Max (°C)
DIESEL	128	283.24	7.92	184.5
JOME	220	470.02	8.44	267.52
B20 JOME	128	376.96	13.56	181.965

Table 7. Combustion characteristics of diesel, JOME, and B20 JOME.

Sample	Ignition Index Di $\times 10^{-4}$ (wt% min^{-1} °C^{-2})	Burnout Index Db $\times 10^{-6}$ (wt% min^{-1} °C^{-3})	Combustion Index Parameter S $\times 10^{-6}$ (wt% min^{-2} °C^{-3})	Intensity of Combustion
DIESEL	3.35	3.35	41.6	0.467
JOME	1.43	6.87	77.74	0.591
B20 JOME	5.82	4.6	57.33	0.318

9. Conclusions

Thermal analysis techniques (TGA and DSC) are useful tools for assessing biodiesels and their derivatives' thermal stability and combustion behavior. It will be useful to determine the samples' stability for enhancing storage conditions prior to engine testing. When biodiesels are blended with diesel, each sample presents new characteristics. Transport properties also play a major role in assessing combustion behavior:

➢ High-enthalpy biodiesels burn inadequately in engines due to poor fuel atomization. The initial endothermic reaction can be attributed to the fuel preparation stage for combustion.

➢ The samples' thermal stability is listed in the following order: oil > biodiesel > blend > diesel.

➢ Larger oil molecules cause a significant difference in stability. Triglycerides are what make up oil. Fatty acids make up biodiesel fuel. The blend TG-DTG curve resembles that of diesel, but with a lower maximum decomposition temperature.

This phenomenon is due to the release of low-molecular-weight compounds in diesel and the interaction of other fuels in the blend. Biodiesel blends reduce the activation energy at the end of the thermal process. Thus, biodiesel has a favorable effect on combustion performance. Thermal degradation for biodiesel takes place in three stages, whereas two stages occur for diesel and blends. Therefore, biodiesel represents a better combustion index. In engines, this leads to hard burning, justifying the high intensity of combustion. Diesel and B20 JOME degradation start from 40 °C, whereas JOME degradation starts from 140 °C. JOME presents more decomposition steps with high decomposition temperatures, indicative of the formation of more stable compounds due to the oxidation process. The peak temperatures of combustion for diesel, JOME, and B20 JOME are 250.4 °C, 292.1 °C, and 266.5 °C, respectively. The ignition index for the B-20 blend is 73.73% more than that of diesel. The combustion index for the B20 blend is 37.81% higher than diesel. The B20 blend exhibits high enthalpy, better thermal stability, and a reduced peak temperature of combustion with an improved combustion index and an intensity of combustion nearly comparable to diesel.

Studies on fuel samples in the environment will be useful to combustion researchers to minimize emissions. Biodiesel blends have a wide range of offset temperatures, followed by diesel. Biodiesel has more decomposition steps. High decomposition temperatures produce additional stable compounds in the oxidation process. Blends' combustion profile is in line with diesel, and they produce minimal emissions of hazardous gases. DSC and TG-DTG are useful tools for assessing the thermal stability and combustion behavior of fuels, either solid or liquid. It will be useful to determine the samples' stability to enhance the storage conditions prior to actual testing, thereby minimizing bench studies. Future studies will be directed towards analyzing the combustion and pyrolysis behavior by performing experiments in different atmospheres with different heating rates for a variety of biofuels and their blends. Similar studies can also be performed for various bio-feed stocks.

References

1. Salvi, B.; Panwar, N. Biodiesel resources and production technologies–A review. *Renew. Sustain. Energy Rev.* **2012**, *16*, 3680–3689. [CrossRef]

2. Wu, G.; Ge, J.C.; Choi, N.J. A Comprehensive Review of the Application Characteristics of Biodiesel Blends in Diesel Engines. *Appl. Sci.* **2020**, *10*, 8015. [CrossRef]

3.   Mahlia, T.M.I.; Syazmi, Z.A.H.S.; Mofijur, M.; Abas, A.E.P.; Bilad, M.R.; Ong, H.C.; Silitonga, A.S. Patent landscape review on biodiesel production: Technology updates. *Renew. Sustain. Energy Rev.* **2020**, *118*, 109526. [CrossRef]

4.   Tamilselvan, P.; Nallusamy, N.; Rajkumar, S. A comprehensive review on performance, combustion and emission characteristics of biodiesel fuelled diesel engines. *Renew. Sustain. Energy Rev.* **2017**, *79*, 1134–1159. [CrossRef]

5.   Kumar, N.; Varun; Chauhan, S.R. Performance and emission characteristics of biodiesel from different origins: A review. *Renew. Sustain. Energy Rev.* **2013**, *21*, 633–658. [CrossRef]

6.   Mohamed, M.; Tan, C.-K.; Fouda, A.; Gad, M.; Abu-Elyazeed, O.; Hashem, A.-F. Diesel Engine Performance, Emissions and Combustion Characteristics of Biodiesel and Its Blends Derived from Catalytic Pyrolysis of Waste Cooking Oil. *Energies* **2020**, *13*, 5708. [CrossRef]

7.   Serrano, M.; Martínez, M.; Aracil, J. Long term storage stability of biodiesel: Influence of feedstock, commercial additives and purification step. *Fuel Process. Technol.* **2013**, *116*, 135–141. [CrossRef]

8.   Saluja, R.K.; Kumar, V.; Sham, R. Stability of biodiesel–A review. *Renew. Sustain. Energy Rev.* **2016**, *62*, 866–881. [CrossRef]

9.   Beatrice, C.; Di Blasio, G.; Lazzaro, M.; Cannilla, C.; Bonura, G.; Frusteri, F.; Asdrubali, F.; Baldinelli, G.; Presciutti, A.; Fantozzi, F.; et al. Technologies for energetic exploitation of biodiesel chain derived glycerol: Oxy-fuels production by catalytic conversion. *Appl. Energy* **2013**, *102*, 63–71. [CrossRef]

10.   International Energy Agency. *Global Energy Review 2019*; IEA: Paris, France, 2020.

11.   Mohsin, R.; Majid, Z.; Shihnan, A.; Nasri, N.; Sharer, Z. Effect of biodiesel blends on engine performance and exhaust emission for diesel dual fuel engine. *Energy Convers. Manag.* **2014**, *88*, 821–828. [CrossRef]

12.   Seela, C.R.; Sankar, B.R.; Kiran, D.S. Influence of biodiesel and its blends on CI engine performance and emissions: A review. *Biofuels* **2016**, *8*, 163–179. [CrossRef]

13.   Peng, D.-X. Exhaust emission characteristics of various types of biofuels. *Adv. Mech. Eng.* **2015**, *7*, 1687814015593036. [CrossRef]

14.   Sáez-Bastante, J.; Pinzi, S.; Reyero, I.; Priego-Capote, F.; de Castro, M.D.L.; Dorado, M.P. Biodiesel synthesis from saturated and unsaturated oils assisted by the combination of ultrasound, agitation and heating. *Fuel* **2014**, *131*, 6–16. [CrossRef]

15.   Jafarihaghighi, F.; Ardjmand, M.; Hassani, M.S.; Mirzajanzadeh, M.; Bahrami, H. Effect of Fatty Acid Profiles and Molecular Structures of Nine New Source of Biodiesel on Combustion and Emission. *ACS Omega* **2020**, *5*, 16053–16063. [CrossRef] [PubMed]

16.   Martínez, G.; Sánchez, N.; Encinar, J.M.; González, J.F. Fuel properties of biodiesel from vegetable oils and oil mixtures. Influence of methyl esters distribution. *Biomass Bioenergy* **2014**, *63*, 22–32. [CrossRef]

17.   Gopinath, A.; Puhan, S.; Nagarajan, G. Effect of unsaturated fatty acid esters of biodiesel fuels on combustion, performance and emission characteristics of a DI diesel engine. *Int. J. Energy Environ.* **2010**, *1*, 411–430.

18.   Benjumea, P.; Agudelo, J.R.; Agudelo, A.F. Effect of the Degree of Unsaturation of Biodiesel Fuels on Engine Performance, Combustion Characteristics, and Emissions. *Energy Fuels* **2011**, *25*, 77–85. [CrossRef]

19.   Zhang, R.; Pham, P.; Kook, S.; Masri, A. Influence of biodiesel carbon chain length on in-cylinder soot processes in a small bore optical diesel engine. *Fuel* **2018**, *235*, 1184–1194. [CrossRef]

20.   Barnwal, B.; Sharma, M. Prospects of biodiesel production from vegetable oils in India. *Renew. Sustain. Energy Rev.* **2005**, *9*, 363–378. [CrossRef]

21.   Agarwal, A.K. Biofuels (alcohols and biodiesel) applications as fuels for internal combustion engines. *Prog. Energy Combust. Sci.* **2007**, *33*, 233–271. [CrossRef]

22.   Sivakumar, P.; Anbarasu, K.; Renganathan, S. Bio-diesel production by alkali catalyzed transesterification of dairy waste scum. *Fuel* **2011**, *90*, 147–151. [CrossRef]

23.   Srikanth, H.; Venkatesh, J.; Godiganur, S.; Manne, B. Acetone and Diethyl ether: Improve cold flow properties of Dairy Washed Milkscum biodiesel. *Renew. Energy* **2019**, *130*, 446–451. [CrossRef]

24.   Meher, L.C.; Naik, S.N.; Das, L.M. Methanolysis of *Pongamia pinnata* (karanja) oil for production of biodiesel. *J. Sci. Ind. Res.* **2004**, *63*, 913–918.

25.   Banapurmath, N.R.; Tewari, P.G.; Hosmath, R.S. Combustion and emission characteristics of a direct injection, compression-ignition engine when operated on honge oil, HOME and blends of HOME and diesel. *Int. J. Sustain. Eng.* **2008**, *1*, 80–93.

26.   Kuti, O.A.; Zhu, J.; Nishida, K.; Wang, X.; Huang, Z. Characterization of spray and combustion processes of biodiesel fuel injected by diesel engine common rail system. *Fuel* **2012**, *104*, 838–846. [CrossRef]

27.   Lin, R.; Tavlarides, L.L. Thermal stability and decomposition of diesel fuel under subcritical and supercritical conditions. *J. Supercrit. Fluids* **2013**, *75*, 101–111. [CrossRef]

28.   Seames, W.; Luo, Y.; Ahmed, I.; Aulich, T.; Kubátová, A.; Šťávová, J.; Kozliak, E. The thermal cracking of canola and soybean methyl esters: Improvement of cold flow properties. *Biomass- Bioenergy* **2010**, *34*, 939–946. [CrossRef]

29.   Shin, H.-Y.; Lim, S.-M.; Bae, S.-Y.; Oh, S.C. Thermal decomposition and stability of fatty acid methyl esters in supercritical methanol. *J. Anal. Appl. Pyrolysis* **2011**, *92*, 332–338. [CrossRef]

30.   Osmont, A.; Catoire, L.; Dagaut, P. Thermodynamic data for the modeling of the thermal decomposition of biodiesel. 1. Saturated and monounsaturated FAMEs. *J. Phys. Chem. A* **2010**, *114*, 3788–3795. [CrossRef]

31.   Hoekman, S.K.; Broch, A.; Robbins, C.; Ceniceros, E.; Natarajan, M. Review of biodiesel composition, properties, and specifications. *Renew. Sustain. Energy Rev.* **2012**, *16*, 143–169. [CrossRef]

32.   Pinzi, S.; Rounce, P.; Herreros, J.M.; Tsolakis, A.; Dorado, M.P. The effect of biodiesel fatty acid composition on combustion and diesel engine exhaust emissions. *Fuel* **2013**, *104*, 170–182. [CrossRef]

33. Coniglio, L.; Bennadji, H.; Glaude, P.A.; Herbinet, O.; Billaud, F. Combustion chemical kinetics of biodiesel and related compounds (methyl and ethyl esters): Experiments and modeling–Advances and future refinements. *Prog. Energy Combust. Sci.* **2013**, *39*, 340–382. [CrossRef]

34. Anitescu, G.; Bruno, T.J. Liquid Biofuels: Fluid Properties to Optimize Feedstock Selection, Processing, Refining/Blending, Storage/Transportation, and Combustion. *Energy Fuels* **2012**, *26*, 324–348. [CrossRef]

35. Oliveira Cordeiro, D.; Gondim, A.D.; Araújo, A.S.; da Conceição, M.M.; de Souza, A.G.; Fernandes, V.J., Jr. Influence of the purification process on the stability of *Jatropha curcas* biodiesel. *J. Therm. Anal. Calorim.* **2017**, *127*, 1253–1260. [CrossRef]

36. Goodrum, J. Volatility and boiling points of biodiesel from vegetable oils and tallow. *Biomass Bioenergy* **2002**, *22*, 205–211. [CrossRef]

37. Knothe, G. Dependence of biodiesel fuel properties on the structure of fatty acid alkyl esters. *Fuel Process. Technol.* **2005**, *86*, 1059–1070. [CrossRef]

38. Lai, J.Y.; Lin, K.; Violi, A. Biodiesel combustion: Advances in chemical kinetic modeling. *Prog. Energy Combust. Sci.* **2011**, *37*, 1–14. [CrossRef]

39. Kohse-Höinghaus, K.; Oßwald, P.; Cool, T.A.; Kasper, T.; Hansen, N.; Qi, F.; Westbrook, C.K.; Westmoreland, P.R. Biofuel Combustion Chemistry: From Ethanol to Biodiesel. *Angew. Chem. Int. Ed.* **2010**, *49*, 3572–3597. [CrossRef]

40. Saggese, C.; Frassoldati, A.; Cuoci, A.; Faravelli, T.; Ranzi, E. A lumped approach to the kinetic modeling of pyrolysis and combustion of biodiesel fuels. *Proc. Combust. Inst.* **2013**, *34*, 427–434. [CrossRef]

41. Liu, T.; Jiaqiang, E.; Yang, W.; Hui, A.; Cai, H. Development of a skeletal mechanism for biodiesel blend surrogates with varying fatty acid methyl esters proportion. *Appl. Energy* **2016**, *162*, 278–288. [CrossRef]

42. Li, A.; Ji, W.; Huang, Z.; Zhu, L. Predictions of oxidation and autoignition of large methyl ester with small molecule fuels. *Fuel* **2019**, *251*, 162–174. [CrossRef]

43. Zettervall, N.; Fureby, C.; Nilsson, E. A reduced chemical kinetic reaction mechanism for kerosene-air combustion. *Fuel* **2020**, *269*, 117446. [CrossRef]

44. Zettervall, N.; Fureby, C.; Nilsson, E.J.K. Small Skeletal Kinetic Reaction Mechanism for Ethylene–Air Combustion. *Energy Fuels* **2017**, *31*, 14138–14149. [CrossRef]

45. Westbrook, C.K.; Pitz, W.J.; Sarathy, S.M.; Mehl, M. Detailed chemical kinetic modeling of the effects of C=C double bonds on the ignition of biodiesel fuels. *Proc. Combust. Inst.* **2013**, *34*, 3049–3056. [CrossRef]

46. Wang, W.; Gowdagiri, S.; Oehlschlaeger, M.A. The high-temperature autoignition of biodiesels and biodiesel components. *Combust. Flame* **2014**, *161*, 3014–3021. [CrossRef]

47. Hoffmann, J.-F.; Henry, J.-F.; Vaitilingom, G.; Olives, R.; Chirtoc, M.; Caron, D.; Py, X. Temperature dependence of thermal conductivity of vegetable oils for use in concentrated solar power plants, measured by 3omega hot wire method. *Int. J. Therm. Sci.* **2016**, *107*, 105–110. [CrossRef]

48. Turgut, A.; Tavman, I.; Tavman, S. Measurement of Thermal Conductivity of Edible Oils Using Transient Hot Wire Method. *Int. J. Food Prop.* **2009**, *12*, 741–747. [CrossRef]

49. Fasina, O.; Colley, Z. Viscosity and Specific Heat of Vegetable Oils as a Function of Temperature: 35 °C to 180 °C. *Int. J. Food Prop.* **2008**, *11*, 738–746. [CrossRef]

50. Simion, A.; Grigoraş, C.-G.; Gavrilă, L. Mathematical modelling of ten vegetable oils thermophysical properties. Study of density and viscosity. *Ann. Food Sci. Technol.* **2014**, *15*, 371–386.

51. Lima Neto, E.G.; Silva, G.P.; Silva, G.F. Evaluation of Group-Contribution Methods to Estimate Vegetable Oils and Biodiesel Properties. *Int. J. Eng. Technol.* **2012**, *2*, 1600–1605.

52. Broniarz-Press, L.; Pralat, K. Thermal conductivity of Newtonian and non-Newtonian liquids. *Int. J. Heat Mass Transf.* **2009**, *52*, 4701–4710. [CrossRef]

53. Balderas López, J.A.; Monsivais Alvarado, T.; Gálvez Coyt, G.; Muñoz Diosdado, A.; Díaz Reyes, J. Thermal characterization of vegetable oils by means of photoacoustic techniques. *Rev. Mex. Física* **2013**, *59*, 168–172.

54. Codreanu, C.; Codreanu, N.-I.; Obreja, V.V.N. Experimental Set-Up for The Measurement of The Thermal Conductivity of Liquids. *Rom. J. Inf. Sci. Technol.* **2007**, *10*, 215–231.

55. Turgut, A.; Sauter, C.; Chirtoc, M.; Henry, J.F.; Tavman, S.; Tavman, I.; Pelzl, J. AC hot wire measurement of thermophysical properties of nanofluids with 3ω method. *Eur. Phys. J. Spec. Top.* **2008**, *153*, 349–352. [CrossRef]

56. Tavman, I.; Turgut, A. An investigation on thermal conductivity and viscosity of water based nanofluids. In *Microfluidics Based Microsystems*; NATO Science for Peace and Security Series A: Chemistry and Biology; Springer: Dordrecht, The Netherlands, 2010; pp. 139–162.

57. Tavman, I.; Turgut, A.; Chirtoc, M.; Hadjov, K.; Fudym, O.; Tavman, S. Experimental Study on Thermal Conductivity and Viscosity of Water-Based Nanofluids. *Heat Transf. Res.* **2010**, *41*, 339–351. [CrossRef]

58. Assael, M.J.; Antoniadis, K.D.; Wakeham, W.A. Historical Evolution of the Transient Hot-Wire Technique. *Int. J. Thermophys.* **2010**, *31*, 1051–1072. [CrossRef]

59. Paul, G.; Chopkar, M.; Manna, I.; Das, P.K. Techniques for measuring the thermal conductivity of nanofluids: A review. *Renew. Sustain. Energy Rev.* **2010**, *14*, 1913–1924. [CrossRef]

60. Yusibani, E.; Woodfield, P.L.; Fujii, M.; Shinzato, K.; Zhang, X.; Takata, Y. Application of the Three-Omega Method to Measurement of Thermal Conductivity and Thermal Diffusivity of Hydrogen Gas. *Int. J. Thermophys.* **2009**, *30*, 397–415. [CrossRef]

61. Antoniadis, K.D.; Assael, M.J.; Wakeham, W.A. Transport Properties of Fluids. *Chem. Eng. Chem. Process Technol.* **2009**, 1–15.
62. Mujtaba, M.A.; Cho, H.M.; Masjuki, H.H.; Kalam, M.A.; Ong, H.C.; Gul, M.; Harith, M.H.; Yusoff, M.N.A.M. Critical review on sesame seed oil and its methyl ester on cold flow and oxidation stability. *Energy Rep.* **2020**, *6*, 40–54. [CrossRef]
63. Shancita, I.; Masjuki, H.H.; Kalam, M.A.; Reham, S.S.; Ruhul, A.M.; Monirul, I.M. Evaluation of the characteristics of non-oxidative biodiesels: A FAME composition, thermogravimetric and IR analysis. *RSC Adv.* **2016**, *6*, 8198–8210. [CrossRef]
64. Conceição, M.M.; Fernandes, V.J.; Araújo, A.S.; Farias, M.F.; Santos, I.M.G.; Souza, A.G. Thermal and oxidative degradation of castor oil biodiesel. *Energy Fuels* **2007**, *21*, 1522–1527. [CrossRef]
65. Lai, Y.; Wang, P.; Chen, X.; Yuan, Y.; Rong, J.; Wu, G.; Zhou, Y.; Zhong, L.; Zhang, Y. Study on Volatility of Palm Oil Biodiesel/-10 Petrodiesel by Thermogravimetric Analysis Technique. *Int. J. u- e- Serv. Sci. Technol.* **2016**, *9*, 263–272. [CrossRef]
66. Santos, A.G.D.; Caldeira, V.P.S.; Souza, L.D.; Oliveira, D.S.; Araujo, A.S.; Luz, G.E., Jr. Study of the thermal stability by thermogravimetry for oil, biodiesel and blend (B$_{10}$) of different oilseeds. *J. Therm. Anal. Calorim.* **2016**, *123*, 2021–2028. [CrossRef]
67. Subramanian, K. A Comprehensive Study on Thermal Degdradation of Selective Edible Vegetable Oils By Simultaneous Thermogravimetric and Differential Thermal Analyses. *J. Pharm. Sci. Res.* **2019**, *11*, 3201–3209.
68. Wnorowska, J.; Ciukaj, S.; Kalisz, S. Thermogravimetric Analysis of Solid Biofuels with Additive under Air Atmosphere. *Energies* **2021**, *14*, 2257. [CrossRef]
69. Bică, M.; Cernăianu, C.; Tutunea, D. The Thermogravimetric Analysis of Different Blends of Biodiesel of Rapeseed and Petrodiesel. *Bull. Transilv. Univ. Bras.* **2009**, *2*, 463–466.
70. Dwivedi, G.; Sharma, M.P. Experimental investigation on thermal stability of Pongamia Biodiesel by thermogravimetric analysis. *Egypt. J. Pet.* **2016**, *25*, 33–38. [CrossRef]
71. Czarnocka, J.; Odziemkowska, M. Diesel fuel degradation during storage process. *Chemik* **2015**, *69*, 771–776.
72. Souza, L.T.A.; Mendes, A.A.; de Castro, H.F. Selection of Lipases for the Synthesis of Biodiesel from Jatropha Oil and the Potential of Microwave Irradiation to Enhance the Reaction Rate. *BioMed Res. Int.* **2016**, *2016*, 1404567. [CrossRef]
73. Da Silva, J.C.T.; Gondim, A.D.; Galvão, L.P.F.C.; da Costa Evangelista, J.P.; Araujo, A.S.; Fernandes, V.J., Jr. Thermal stability evaluation of biodiesel derived from sunflower oil obtained through heterogeneous catalysis (KNO$_3$/Al$_2$O$_3$) by thermogravimetry. *J. Therm. Anal. Calorim.* **2015**, *119*, 715–720. [CrossRef]
74. Farias, R.M.C.; Conceição, M.M.; Candeia, R.A.; Silva, M.C.D.; Fernandes, V.J.; Souza, A.G. Evaluation of the thermal stability of biodiesel blends of castor oil and passion fruit. *J. Therm. Anal. Calorim.* **2011**, *106*, 651–655. [CrossRef]
75. Demirbas, A. Thermal Degradation of Fatty Acids in Biodiesel Production by Supercritical Methanol. *Energy Explor. Exploit.* **2007**, *25*, 63–70. [CrossRef]
76. Todaka, M.; Kowhakul, W.; Masamoto, H.; Shigematsu, M.; Onwona-Agyeman, S. Thermal decomposition of biodiesel fuels produced from rapeseed, jatropha, and coffee oils with different alcohols. *J. Therm. Anal. Calorim.* **2013**, *113*, 1355–1361. [CrossRef]
77. Peer, M.S.; Kasimani, R.; Rajamohan, S.; Ramakrishnan, P. Experimental evaluation on oxidation stability of biodiesel/diesel blends with alcohol addition by rancimat instrument and FTIR spectroscopy. *J. Mech. Sci. Technol.* **2017**, *31*, 455–463. [CrossRef]
78. Khurana, D.; Agarwal, A.K. Oxidation Stability, Engine Performance and Emissions Investigations of Karanja, Neem and Jatropha Biodiesel and Blends. *SAE Int. J. Fuels Lubr.* **2011**, *4*, 76–83. [CrossRef]
79. Dunn, R.O. Oxidative Stability of Biodiesel by Dynamic Mode Pressurized-Differential Scanning Calorimetry (P-DSC). *Trans. ASABE* **2006**, *49*, 1633–1641. [CrossRef]
80. Agarwal, A.K.; Khurana, D.; Dhar, A. Improving oxidation stability of biodiesels derived from Karanja, Neem and Jatropha: Step forward in the direction of commercialisation. *J. Clean. Prod.* **2015**, *107*, 646–652. [CrossRef]
81. Shameer, P.M.; Ramesh, K. FTIR evaluation on the fuel stability of calophyllum inophyllum biodiesel: Influence of tert-butyl hydroquinone (TBHQ) antioxidant. *J. Mech. Sci. Technol.* **2017**, *31*, 3611–3617. [CrossRef]
82. Mothé, C.G.; de Castro, B.C.S.; Mothé, M.G. Characterization by TG/DTG/DSC and FTIR of frying and fish oil residues to obtain biodiesel. *J. Therm. Anal. Calorim.* **2011**, *106*, 811–817. [CrossRef]
83. Christensen, E.; McCormick, R.L. Long-term storage stability of biodiesel and biodiesel blends. *Fuel Process. Technol.* **2014**, *128*, 339–348. [CrossRef]
84. Freire, L.; Bicudo, T.; Rosenhaim, R.; Sinfrônio, F.; Botelho, J.; Carvalho Filho, J.; Santos, I.; Fernandes, V.; Antoniosi Filho, N.; Souza, A. Thermal investigation of oil and biodiesel from *Jatropha curcas* L. *J. Therm. Anal. Calorim.* **2009**, *96*, 1029–1033. [CrossRef]
85. Jose, T.K.; Anand, K. Effects of biodiesel composition on its long term storage stability. *Fuel* **2016**, *177*, 190–196. [CrossRef]
86. Macedo, F.L.; Candeia, R.A.; Sales, L.L.M.; Dantas, M.B.; Souza, A.G.; Conceição, M.M. Thermal characterization of oil and biodiesel from oiticica (*Licania rigida* Benth). *J. Therm. Anal. Calorim.* **2011**, *106*, 531–534. [CrossRef]
87. Rashed, M.M.; Kalam, M.A.; Masjuki, H.H.; Rashedul, H.K.; Ashraful, A.M.; Shancita, I.; Ruhul, A.M. Stability of biodiesel, its improvement and the effect of antioxidant treated blends on engine performance and emission. *RSC Adv.* **2015**, *5*, 36240–36261. [CrossRef]
88. Garcia-Perez, M.; Adams, T.T.; Goodrum, J.W.; Das, K.C.; Geller, D.P. DSC studies to evaluate the impact of bio-oil on cold flow properties and oxidation stability of bio-diesel. *Bioresour. Technol.* **2010**, *101*, 6219–6224. [CrossRef] [PubMed]
89. Nair, J.; Satyanarayana Murthy, Y.V.V.; Ramesh, M. Synthesis of Algae Biodiesel Using K$_2$CO$_3$/ZnO Heterogeneous Base Catalyst and Its Characterisation. *Rasayan J. Chem.* **2019**, *12*, 1757–1765. [CrossRef]

90. Al-Samaraae, R.R.; Atabani, A.E.; Uguz, G.; Kumar, G.; Arpa, O.; Ayanoglu, A.; Mohammed, M.N.; Farouk, H. Perspective of safflower (*Carthamus tinctorius*) as a potential biodiesel feedstock in Turkey: Characterization, engine performance and emissions analyses of butanol–biodiesel–diesel blends. *Biofuels* **2020**, *11*, 715–731.

91. Leonardo, R.S.; Valle, M.L.M.; Dweck, J. Thermovolumetric and thermogravimetric analysis of diesel S_{10}. Comparison with ASTM D86 standard method. *J. Therm. Anal. Calorim.* **2020**, *139*, 1507–1514. [CrossRef]

92. Stenseng, M.; Zolin, A.; Cenni, R.; Frandsen, F.; Jensen, A.; Dam-Johansen, K. Thermal Analysis in Combustion Research. *J. Therm. Anal. Calorim.* **2001**, *64*, 1325–1334. [CrossRef]

93. Malvis, A.; Šimon, P.; Dubaj, T.; Sládková, A.; Ház, A.; Jablonský, M.; Sekretár, S.; Schmidt, Š.; Kreps, F.; Burčová, Z.; et al. Determination of the Thermal Oxidation Stability and the Kinetic Parameters of Commercial Extra Virgin Olive Oils from Different Varieties. *J. Chem.* **2019**, *2019*, 4567973. [CrossRef]

94. De Robertis, E.; Moreira, G.F.; Silva, R.A.; Achete, C.A. Thermal behavior study of biodiesel standard reference materials. *J. Therm. Anal.* **2011**, *106*, 347–354. [CrossRef]

95. Melo, M.A.M.F.; de Melo, M.A.R.; Pontes, A.S.G.C.; Farias, A.F.F.; Dantas, M.B.; Calixto, C.D.; de Souza, A.G.; de Carvalho Filho, J.R. Non-conventional oils for biodiesel production: A study of thermal and oxidative stability. *J. Therm. Anal. Calorim.* **2014**, *117*, 845–849. [CrossRef]

96. Ramalho, E.F.S.M.; dos Santos, I.M.G.; Maia, A.S.; Souza, A.L.; Souza, A.G. Thermal characterization of the poultry fat biodiesel. *J. Therm. Anal.* **2011**, *106*, 825–829. [CrossRef]

97. Santos, O.V.; Correa, N.C.F.; Junior, R.C.; da Costa, C.E.F.; de Fátima Cabral Moraes, J.; da Silva Lannes, S.C. Quality parameters and thermogravimetric and oxidative profile of Muruci oil (*Byrsonima crassifolia* L.) obtained by supercritical CO_2. *Food Sci. Technol.* **2018**, *38*, 172–179.

98. Donoso, D.; Bolonio, D.; Lapuerta, M.; Canoira, L. Oxidation Stability: The Bottleneck for the Development of a Fully Renewable Biofuel from Wine Industry Waste. *ACS Omega* **2020**, *5*, 16645–16653. [CrossRef]

99. Borugadda, V.B.; Goud, V.V. Comparative studies of thermal, oxidative and low temperature properties of waste cooking oil and castor oil. *J. Renew. Sustain. Energy* **2013**, *5*, 063104. [CrossRef]

100. Misutsu, M.Y.; Cavalheiro, L.F.; Ricci, T.G.; Viana, L.H.; de Oliveira, S.C.; Junior, A.M.; de Oliveira, L.C. Thermoanalytical Methods in Verifying the Quality of Biodiesel. In *Biofuels—Status and Perspective*; Intech: Rijeka, Croatia, 2015; pp. 251–269.

101. Alaba, P.A.; Sani, Y.M.; Daud, W.M.A.W. A comparative study on thermal decomposition behavior of biodiesel samples produced from shea butter over micro- and mesoporous ZSM-5 zeolites using different kinetic models. *J. Therm. Anal. Calorim.* **2016**, *126*, 943–948. [CrossRef]

102. De Morais, L.C.; Santos, C.M.; Rosa, A.H. Thermodynamic Parameters of a Solid Biofuel from Orange Peel. *Chem. Eng. Trans.* **2015**, *43*, 583–588.

103. Lai, Y.; Wang, B.; Chen, X.; Yuan, Y.; Zhong, L.; Qiao, X.; Zhang, Y.; Yuan, M.; Shu, J.; Wang, P. Thermogravimetric analysis of combustion characteristics of palm oil and rapeseed oil biodiesel. *Biotechnology* **2015**, *14*, 9–15. [CrossRef]

104. Andrade, R.D.A.; Pozzebom, E.; Faria, E.A.; Filho, F.D.; Suarez, P.A.Z.; do Prado, A.G.S. Thermal behavior of diesel/biodiesel blends of biodiesel obtained from buriti oil. *Acta Sci.* **2012**, *34*, 243–248. [CrossRef]

105. Li, H.; Niu, S.; Lu, C.; Wang, Y. Comprehensive Investigation of the Thermal Degradation Characteristics of Biodiesel and Its Feedstock Oil through TGA–FTIR. *Energy Fuels* **2015**, *29*, 5145–5153. [CrossRef]

106. Volli, V.; Purkait, M.K. Physico-chemical properties and thermal degradation studies of commercial oils in nitrogen atmosphere. *Fuel* **2014**, *117*, 1010–1019. [CrossRef]

107. Imdadul, H.; Masjuki, H.; Kalam, A.; Zulkifli, N.; Alabdulkarem, A.; Rashed, M.; Ashraful, A. Influences of ignition improver additive on ternary (diesel-biodiesel-higher alcohol) blends thermal stability and diesel engine performance. *Energy Convers. Manag.* **2016**, *123*, 252–264. [CrossRef]

108. Wang, Y.L.; Lee, D.J.; Westbrook, C.K.; Egolfopoulos, F.N.; Tsotsis, T.T. Oxidation of small alkyl esters in flames. *Combust. Flame* **2014**, *161*, 810–817. [CrossRef]

109. Bezerra Mota Gomes Arruda, T.; Arruda Rodrigues, F.E.; Duarte Arruda, D.T.; Pontes Silva Ricardo, N.M.; Barbosa Dantas, M.; de Araújo, K.C. Chromatography, spectroscopy and thermal analysis of oil and biodiesel of sesame (*Sesamum indicum*)−An alternative for the Brazilian Northeast. *Ind. Crops Prod.* **2016**, *91*, 264–271. [CrossRef]

110. Kok, M.V. Use of thermal equipment to evaluate crude oils. *Thermochim. Acta* **1993**, *214*, 315–324. [CrossRef]

111. De Andrade Ávila, R.N.; Sodre, J.R. Physical–chemical properties and thermal behavior of fodder radish crude oil and biodiesel. *Ind. Crop. Prod.* **2012**, *38*, 54–57. [CrossRef]

112. Borsato, D.; Galvan, D.; Pereira, J.L.; Orives, J.R.; Angilelli, K.G.; Coppo, R.L. Kinetic and Thermodynamic Parameters of Biodiesel Oxidation with Synthetic Antioxidants: Simplex Centroid Mixture Design. *J. Braz. Chem. Soc.* **2014**, *25*, 1984–1992. [CrossRef]

113. Andrade, R.D.A.; Faria, E.A.; Silva, A.M.; Araujo, W.C.; Jaime, G.C.; Costa, K.P.; Prado, A.G.S. Heat of combustion of biofuels mixed with fossil diesel oil. *J. Therm. Anal. Calorim.* **2011**, *106*, 469–474. [CrossRef]

114. Bezerra Mota Gomes Arruda, T.; Barbosa Dantas, M.; de Araújo, K.C.; Arruda Rodrigues, F.E.; Pontes Silva Ricardo, N.M.; Bitu, S.G. Blends of diesel and biodiesel of cooking oil waste and moringa (*Moringa oleífera* Lam): Kinetic and thermal analysis and monitoring during storage. *Int. J. Energy Environ. Eng.* **2017**, *8*, 135–141. [CrossRef]

115. Conconi, C.C.; Crnkovic, P.M. Thermal behavior of renewable diesel from sugar cane, biodiesel, fossil diesel and their blends. *Fuel Process. Technol.* **2013**, *114*, 6–11. [CrossRef]

116. Crnkovic, P.M.; Leiva, C.R.M.; dos Santos, A.M.; Milioli, F.E. Kinetic Study of the Oxidative Degradation of Brazilian Fuel Oils. *Energy Fuels* **2007**, *21*, 3415–3419. [CrossRef]
117. Jain, S.; Sharma, M. Oxidation and thermal behavior of *Jatropha curcas* biodiesel influenced by antioxidants and metal contaminants. *Int. J. Eng. Sci. Technol.* **2011**, *3*, 65–75. [CrossRef]
118. Mortari, D.A.; Avila, I.; dos Santos, A.M.; Crnkovic, P.M. Study of thermal decomposition and ignition temperature of bagasse, coal and their blends. *Rev. Eng. Térmica* **2010**, *9*, 81–88. [CrossRef]
119. Xing, X.; Wang, S.; Zhang, Q. Thermogravimetric Analysis and Kinetics of Mixed Combustion of Waste Plastics and Semicoke. *J. Chem.* **2019**, *2019*, 8675986. [CrossRef]
120. Song, C.-Z.; Wen, J.-H.; Li, Y.-Y.; Dan, H.; Shi, X.-Y.; Xin, S. Thermogravimetric Assessment of Combustion Characteristics of Blends of Lignite Coals with Coal Gangue. *Adv. Eng. Res.* **2017**, *105*, 490–495.
121. Kok, M.V.; Topa, E. Combustion characteristics and kinetics of diesel and canola oil samples. *Energy Sources Part A-Recovery Util. Environ. Eff.* **2016**, *38*, 967–974. [CrossRef]
122. Liu, S.; Chen, M.; Hu, Q.; Wang, J.; Kong, L. The kinetics model and pyrolysis behavior of the aqueous fraction of bio-oil. *Bioresour. Technol.* **2013**, *129*, 381–386. [CrossRef]
123. Soto, F.; Alves, M.; Valdés, J.C.; Armas, O.; Crnkovic, P.; Rodrigues, G.; Lacerda, A.; Melo, L. The determination of the activation energy of diesel and biodiesel fuels and the analysis of engine performance and soot emissions. *Fuel Process. Technol.* **2018**, *174*, 69–77. [CrossRef]
124. Ninduangdee, P.; Kuprianov, V.I.; Cha, E.Y.; Kaewrath, R.; Youngyuen, P.; Atthawethworawuth, W. Thermogravimetric Studies of Oil Palm Empty Fruit Bunch and Palm Kernel Shell: TG/DTG Analysis and Modeling. *Energy Procedia* **2015**, *79*, 453–458. [CrossRef]
125. Wang, L.; Xiu, S.; Shahbazi, A. Combustion characteristics of bio-oil from swine manure/crude glycerol co-liquefaction by thermogravimetric analysis technology. *Energy Sources Part A Recovery Util. Environ. Eff.* **2016**, *38*, 2250–2257. [CrossRef]
126. Samad, J.; Zehni, A. Combustion modeling for modern direct injection diesel engines. *Iran. J. Chem. Chem. Eng.* **2012**, *31*, 111–114.
127. Raj, R.T.K.; Manimaran, R. Effect of Swirl in a Constant Speed DI Diesel Engine using Computational Fluid Dynamics. *CFD Lett.* **2012**, *4*, 214–224.
128. Baratta, M.; Chiriches, S.; Goel, P.; Misul, D. CFD modelling of natural gas combustion in IC engines under different EGR dilution and H2-doping conditions. *Transp. Eng.* **2020**, *2*, 100018. [CrossRef]
129. Costa, M.; Piazzullo, D. Biofuel Powering of Internal Combustion Engines: Production Routes, Effect on Performance and CFD Modeling of Combustion. *Front. Mech. Eng.* **2018**, *4*, 9. [CrossRef]
130. Maghbouli, A.; Saray, R.K.; Shafee, S.; Ghafouri, J. Numerical study of combustion and emission characteristics of dual-fuel engines using 3D-CFD models coupled with chemical kinetics. *Fuel* **2013**, *106*, 98–105. [CrossRef]
131. Vijayashree; Ganesan, V. Application of CFD for Analysis and Design of IC Engines. In *Advances in Internal Combustion Engine Research*; Energy, Environment, and Sustainability; Springer: Singapore, 2018; pp. 251–306. [CrossRef]
132. Atgur, V.; Manavendra, G.; Desai, G.; Rao, B.N. Experimental investigation on thermal conductivity and thermal degradation of Honge oil methyl ester with B-20 blend. *J. Therm. Eng.* **2021**, *7*, 1604–1613. [CrossRef]
133. Atgur, V.; Manavendra, G.; Desai, G.; Rao, B.N. Thermogravitometry and calorimetric evaluation of honge oil methyl ester and its B-20 blend. *Clean. Eng. Technol.* **2021**, *6*, 100367. [CrossRef]
134. Atgur, V.; Manavendra, G.; Desai, G.; Rao, B.N. Thermal characterisation of dairy washed scum methyl ester and its b-20 blend for combustion applications. *Int. J. Ambient Energy* **2021**, 1–11. [CrossRef]
135. Atgur, V.; Manavendra, G.; Desai, G.P.; Rao, B.N. CFD Combustion Simulations and Experiments on the Blended Biodiesel Two-Phase Engine Flows. In *Computational Fluid Dynamics*; IntechOpen: London, UK, 2022. [CrossRef]
136. Sanjeevannavar, M.B.; Banapurmath, N.; Soudagar, M.E.M.; Atgur, V.; Hossain, N.; Mujtaba, M.; Khan, T.Y.; Rao, B.N.; Ismail, K.A.; Elfasakhany, A. Performance indicators for the optimal BTE of biodiesels with additives through engine testing by the Taguchi approach. *Chemosphere* **2022**, *288*, 132450. [CrossRef] [PubMed]
137. Rajyalakshmi, K.; Boggarapu, N.R. Expected range of the output response for the optimum input parameters utilizing the modified Taguchi approach. *Multidiscip. Modeling Mater. Struct.* **2019**, *15*, 508–522.
138. Atgur, V.; Manavendra, G.; Desai, G.P.; Rao, B.N.; Fattah, I.M.R.; Mohamed, B.A.; Sinaga, N.; Masjuki, H.H. Thermogravimetric and combustion efficiency analysis of *Jatropha curcas* biodiesel and its derivatives. *Biofuels* **2022**, 1–11. [CrossRef]